AFIT/GNE/PH/82M-6

CATHODOLUMINESCENCE AND PHOTOLUMINESCENCE STUDY OF SILICON IMPLANTED GALLIUM ARSENIDE

THESIS

AFIT/GNE/PH/82M-6 Daniel L. DeForest
2LT USAF

Approved for public release; distribution unlimited

AFIT/GNE/PH/82M-6

CATHODOLUMINESCENCE AND PHOTOLUMINESCENCE STUDY OF SILICON IMPLANTED GALLIUM ARSENIDE

THESIS

Presented to the Faculty of the School of Engineering

of the Air Force Institute of Technology

Air University

in Partial Fulfillment of the

Requirements for the Degree of

Master of Science

by

Daniel L. DeForest
2LT USAF

Graduate Nuclear Engineering

March 1982

Preface

The completion of this thesis proved to be a very worthwhile learning experience. In addition to providing valuable experience in confronting unique problems, this study served to instill an attitude towards the approach of any problem. However, this thesis would not have been possible without the help of several individuals. Among them I would like to thank Dr. Robert L. Hengehold, my thesis advisor, for his advice and guidance throughout the work of this thesis. I would also like to thank Jim Miskimen for his help and patience in putting a working system together. Additional thanks go to Ron Gabriel and George Gergal of the AFIT Physics Laboratory for their technical assistance. My thanks also go out to AFWAL/AADR, Wright-Patterson AFB, Ohio for providing the samples used in this study. Finally, I would like to thank my wife, Paula, who had to "Grin and Bear it" during this hectic period.

Daniel L. DeForest

(This thesis was typed by Paula DeForest)

Contents

List of Figures

List of Tables

Abstract

Depth resolved photoluminescence and cathodoluminescence data were obtained from gallium arsenide implanted with 120 keV silicon ions. The luminescence data were studied as a function of depth in an effort to determine the implant damage profile of the silicon in GaAs. A chemical etchant was used to etch off successive layers of the crystal surface. The substrate material used for this study was bulk GaAs, grown by the Liquid-Encapsulated Czochralski (LEC) method.

The data from both photo- and cathodoluminescence indicated that the extent of damage produced in the samples increased with increasing dosage. This is supported by similar studies involving implanted GaAs. Additionally, a "dead" layer, in which all cathodoluminescence was completely quenched, was observed extending up to depths of 3500 Å into the samples. Correlation of the data from all implanted samples indicated that either some diffusion of defects had occurred or that the theory predicting the implant profile is flawed.

CATHODOLUMINESCENCE AND PHOTOLUMINESCENCE STUDY OF SILICON IMPLANTED GALLIUM ARSENIDE

I. Introduction

The semiconductor materials which are presently being used by commercial industry are not appropriate for current and future defense applications which require specialized high speed electronics. Additionally, many defense systems are now required to operate in high temperature environments where conventional semiconductor materials break down (Ref 1). Gallium arsenide, because of its higher electron mobility and wider band gap, looks promising for use in these areas (Refs 13:325; 23:371).

In its standard state gallium arsenide (GaAs) is a crystalline material made up of a Group III element, gallium, and a Group V element, arsenic. Its physical properties are very similar to the Group IV elements (such as silicon) with the exception of its slight ionic character which accounts for its higher electron mobility. It also has a wider direct band gap which improves its stability at higher temperatures. Unfortunately, pure GaAs (intrinsic) must be properly doped with an impurity (extrinsic) before attaining useful semiconducting properties.

Often the most common methods of doping, such as diffusion, involve elevating the sample to high temperatures (on the order of 1000°C). For GaAs these methods are not effective since arsenic's higher vapor pressure causes depletion of the arsenic in the crystal

during the process. One method of doping which has already proven to be successful in the production of field effect transistors, integrated circuits, microwave devices, and optoelectronic devices is ion implantation. Not only can this technique be 1) performed at room temperature but 2) very high purity ions can be introduced into the crystal and 3) the doping profile can be controlled accurately in three dimensions by varying the energy, size, and position of the beam (Ref 24:627). Unfortunately, there is an important disadvantage of ion implantation. The impingement of the particles (ions) onto the crystal surface displaces and replaces some of the resident lattice atoms through collisions. As a result the semiconducting properties of the target material may be degraded immensely. Annealing the crystal can "activate" the implanted ions and restore some of the lost properties. This still may not remove all the damage however (Ref 21). In order to fully understand the effect of damage on the properties of GaAs, the profile of damage in the material and the type of damage introduced need to be fully characterized.

Luminescence is a convenient diagnostic tool to use in this characterization because of its dependence on energy levels. Luminescence involves the production of electron-hole pairs and their subsequent radiative recombination. Since the probability of a particular recombination occurring depends on the relative proportion of the energy levels allowing the transition, the intensity of the resulting liminescence will be a function of the concentration of the element(s) which provide the energy levels. The electron-hole pairs can be produced by exciting the electrons to a higher energy level with either photons (photoluminescence) or high energy electrons

(cathodoluminescence) (Ref 6). By studying the liminescence spectra as layers of the material are etched away, the effects of damage and/or impurities should be observed as a function of depth into the crystal. From these observations a depth profile of damage can be derived.

The objective of this study was to investigate the effects of damage in GaAs from ion implantation as a function of depth. Both photoluminescence and cathodoluminescence were used as the diagnostic tools. Silicon was the only implant species used. The samples studied were all GaAs bulk grown by the Liquid-Encapsulated Czochralski (LEC) method. Three samples of GaAs were implanted at ion dosages of 10^{12} cm^{-2}, 10^{13} cm^{-2}, and 10^{15} cm^{-2} respectively. A fourth (control) sample was not implanted. All samples were unannealed. For each sample the photoluminescence and cathodoluminescence spectra were recorded after etching off successive layers of material by chemical means. The normalized magnitudes were then plotted as a function of amount of material etched off to obtain a depth profile of the damage.

II. Theory

To adequately understand the basis for the conclusions reached in the final chapter, basic theory is presented at this point on the various subjects involved in reaching those conclusions. In the information presented, the reader is assumed to have a basic understanding of band theory. Those readers who wish to review basic band theory are referred to the various books on the subject. The major topics appearing in this section are the following: Luminescence, Radiative Recombinations, Ion Implantation, Laser Penetration, and Electron Beam Penetration.

Luminescence

The basic process that produces luminescence was briefly discussed in the Introduction. The electrons present in the lattice can be excited by either photons or electrons. Because the excitation source is attenuated as it penetrates into the sample, it follows that the greatest amount of energy absorption will occur at or near the surface. The electron-hole pairs that are produced will tend to diffuse away from the excited area in order to restore homogeneity. However, because of self absorption of the emitted radiation in these areas and the reduced probability of self absorption in the areas already excited, it follows that the recombination radiation (luminescence) will most readily escape from the sample through the excited surface (Ref 4:182). A more detailed description of the types of electron-hole recombinations which give rise to luminescence will be given in the next section.

Radiative Recombinations

Because electrons and holes can exist in several of the different energy levels in a crystal, the different combinations of the levels available lead to several possible energies being emitted when the excited electrons and holes recombine. These different energies can result in a luminescence spectra involving many lines. Most of the luminescence lines that have been identified in GaAs involve "simple" centers although luminescence can also be associated with "complex" centers.

Simple Center. A simple center can be thought of as an impurity sitting on a lattice site which can be modeled using hydrogen type energy levels. The radiative transitions possible in such a model are demonstrated in Figure 1. Referring to this diagram, line (A) represents the recombination of a free electron and a free hole. The energy of such a transition is given by

$$E(h\nu) = E(Gap) + 2kT \qquad (1)$$

where

$E(h\nu)$ = the energy of the emitted photon

$E(Gap)$ = the energy of the gap between the conduction band and valence band (1.521 eV at 21°K)

k = Boltzmann's constant

T = temperature in degrees Kelvin

In the absence of other effects the effect of the kT term in Eq. (1) is to increase the energy of the emitted photon with increasing temperature. This term is derived from the kinetic energies of the free electron and free hole (Refs 3:1042; 6:7). In reality, the effect

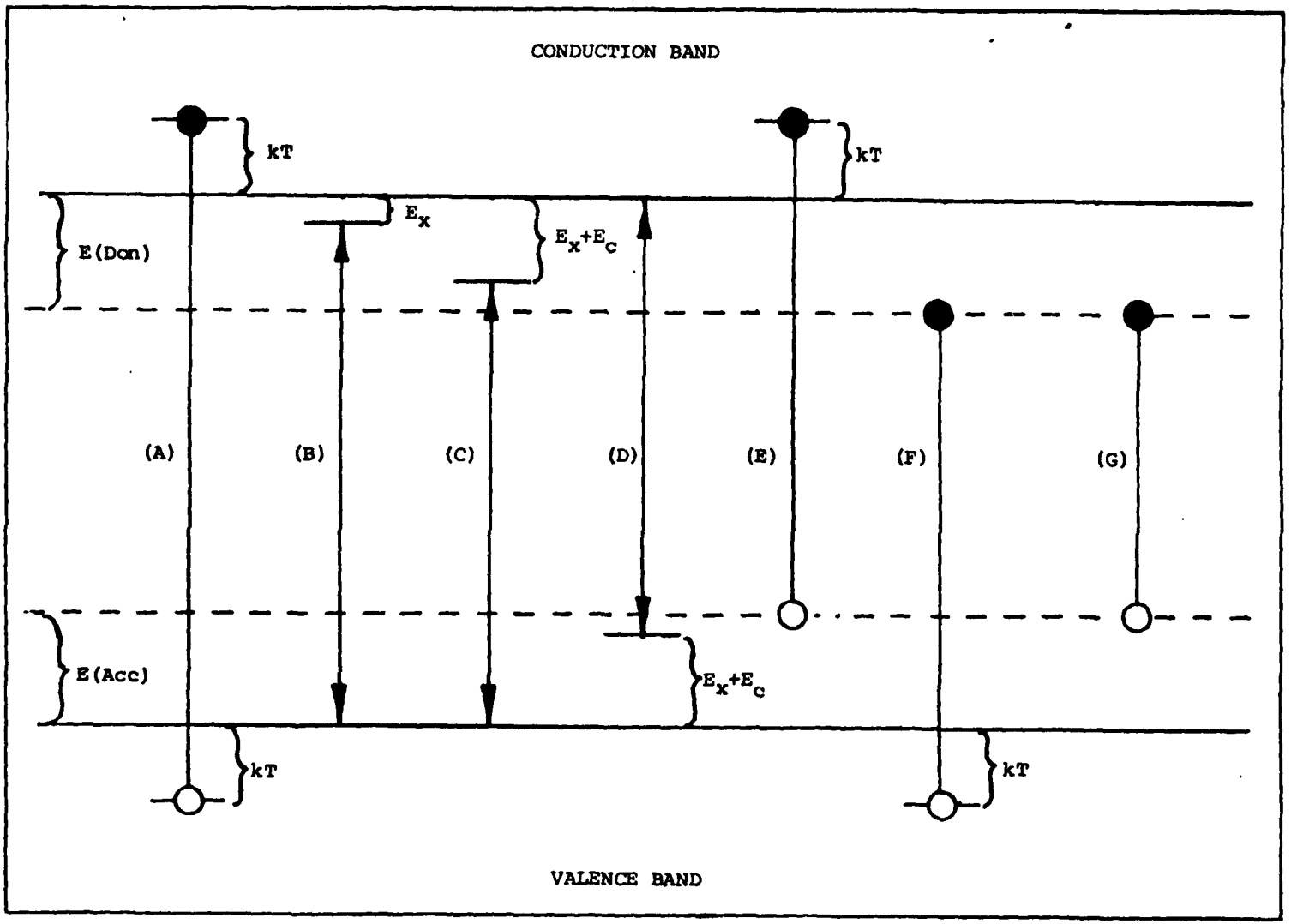

Fig. 1. Simple Energy Band Diagram

of this term can be negated by the simultaneous decrease in band gap energy with increasing temperature. At low temperatures the photon energy is very close to the gap energy. For example at a typical temperature used in this study, 8°K, this increase in energy amounts to only .689 meV (compared to eV's). As of the present, this transition has not been observed in bulk grown GaAs and consequently estimates of the gap energy are currently made from exciton transitions (Ref 31:386).

The (B) line of Fig. 1 represents the recombination of a free exciton. An exciton can be thought of as an electron and a hole which are "bound" to each other through coulombic attraction. A "free" exciton is free to move throughout the lattice. Because the exciton has a slightly reduced energy due to the binding forces involved, the photon emitted has an energy slightly lower than the free electron-free hole pair recombination (Ref 18:504). At 2°K, this emitted energy lies at 1.5156 eV in GaAs (Ref 31:342), slightly less than the band gap energy. Because a free exciton can acquire kinetic energy, the energy of this transition has a thermal dependence connected with it. A method for calculating the energy released during free exciton recombination was elaborated on by Pierce (Ref 27:38).

Line (C) of Fig. 1 represents the recombination of an exciton bound to a donor site, while line (D) represents an exciton bound to an acceptor site. Again, because of the additional binding energy involved with the donor or acceptor, the energy of the emitted photon is less than that of either the free exciton or the free electron-free hole recombinations (Ref 4:299). Since the exciton has no velocity, and therefore no kinetic energy, when bound to an impurity site, the energy of this type of transition does not exhibit a direct thermal

dependence (Ref 27:39). In silicon doped GaAs at 2°K, three bound exciton lines have been reported; 1.5145 eV, 1.5135 eV, and 1.5125 eV (Ref 31:342). Bound exciton emissions generally have slightly narrower lines than the free exciton emission.

Line (E) represents a free electron-bound hole recombination in which the hole is bound to an acceptor. The energy of this type of transition is given by (Ref 8:744):

$$E(h\nu) = E(Gap) - E(Acc) + kT + nE(ph) \qquad (2)$$

where

E(Acc) = acceptor energy level (30 meV for Si in GaAs at 20°K)

n = number of phonons (lattice vibrations) which assist the transition

E(ph) = phonon energy (36 meV for the longitudinal optical phonon in GaAs)

The E(ph) term in Eq. (2) represents the discrete amount of energy that can be given to or absorbed by the crystal through lattice vibrations. Like the free electron-free hole recombination, the energy of this transition exhibits a thermal dependence. But, because only the electron is free, the thermal dependence in Eq. (2) is half that in Eq. (1). Generally differences in energy levels for different acceptors are large enough that acceptor identification can be made. Typical acceptor energies of this type of transition are given in Table 1 (Ref 3:1051; 28:1111).

Line (F) represents the conjugate to line (E), a recombination of a bound electron-free hole where the electron is bound to a donor. In GaAs the energy levels of donors, unlike acceptors, are too close

TABLE 1

TYPICAL CONDUCTION BAND TO BOUND ACCEPTOR TRANSITIONS

Acceptor	Transition Energy eV
Carbon	1.4935, 1.4939
Silicon	1.4850, 1.4902
Germanium	1.4790
Tin	1.3490
Zinc	1.4888
Cadmium	1.4848
Beryllium	1.4915
Magnesium	1.4911

together to be discriminated. Additionally, the intensity of these transitions is usually weak. A peak at 1.5137 eV in GaAs has been attributed to this type of transition (Ref 31:342). An equation similar to Eq. (2) would be used to calculate the energy of the emitted photon, with the energy level and phonon assist energy for the donor being substituted for those of the acceptor.

The last transition, line (G), represents the recombination of a bound electron with a bound hole. The energy of the emitted photon for this transition is given by (Refs 31:335, 8:744)

$$E(h\nu) = E(Gap) - [E(Acc) + E(Don)] + e^2/\varepsilon R \qquad (3)$$

where

e = the charge on an electron

ε = the dielectric constant of the material (GaAs)

R = the spacing between the interacting donor acceptor pair

Because the electron and hole are both bound to impurities and the impurity atoms occupy discrete lattice sites, the energies which are available for emission take on discrete values (the last term in Eq. (3)). It should therefore be possible to see a series of discrete luminescence lines from this transition (Ref 31:335). The intensities of individual lines would also be expected to decrease as R is increased since probability of interaction decreases with increasing distance. In reality the only peak which has been seen from this type of transition in GaAs has been from electrons and holes bound to impurities separated by large distances where the individual lines start to overlap (where $E(h\nu) = E(Gap) - [E(Acc) + E(Don)]$). The observed energy of this peak is located around 1.485 eV at 20°K (Ref 5:1000).

Complex Center. A complex center involves an impurity and/or vacancy "complex" which has an energy level located deep within the gap between the conductor and valence bands. An example of a complex center might be an impurity which is close enough to a vacancy (or another impurity) to interact to form a "complex" having its own properties and energy levels (Ref 30:1663). Because these complexes do not mesh with the periodicity of the lattice and can vary in energy, complex centers can not be modeled with hydrogen type energy levels. Additionally, the luminescent peaks usually observed for complex centers are broad and of low energy. Most complex centers are believed to involve lattice vacancies. Some transition metals and precipitates

have also been associated with complex centers (Ref 31:359).

Ion Implantation

As mentioned in the Introduction, ion implantation has proven to be a successful method of doping GaAs for several reasons (Ref 24:627):

1) the process can be performed at room temperature
2) high purity dopants are attainable
3) an accurate three dimensional profile can be obtained by control of beam energy, beam size, and beam position
4) almost any element can be used as a dopant

The basic process of ion implantation involves choosing a dopant species, purifying the species, ionizing the species, and accelerating the ions towards a sample. The accelerated ions collide with the atoms of the crystal lattice, losing some of their energy with each collision. Eventually, the ions will come to rest when they have lost all of their energy. The amount of energy lost with each collision depends on many factors, i.e. ion type, lattice atom type, lattice density, incident energy and the probability that a collision will occur. This results in a loss of energy per collision which is completely random within the limits of the incident energy of the ion. Because the amount of energy lost will determine how long it takes for a particular ion to lose all its energy, some ions will lose their energy sooner than others. The final product of this is an implant depth profile. The implant profile of 120/keV silicon ions in GaAs (Fig. 2) has been predicted using a range distribution theory developed by Lindhard, Scharff, and Schiott (LSS) (Ref 20). This theory was developed for amorphous materials, but has been applied to crystals as well. The profiles in

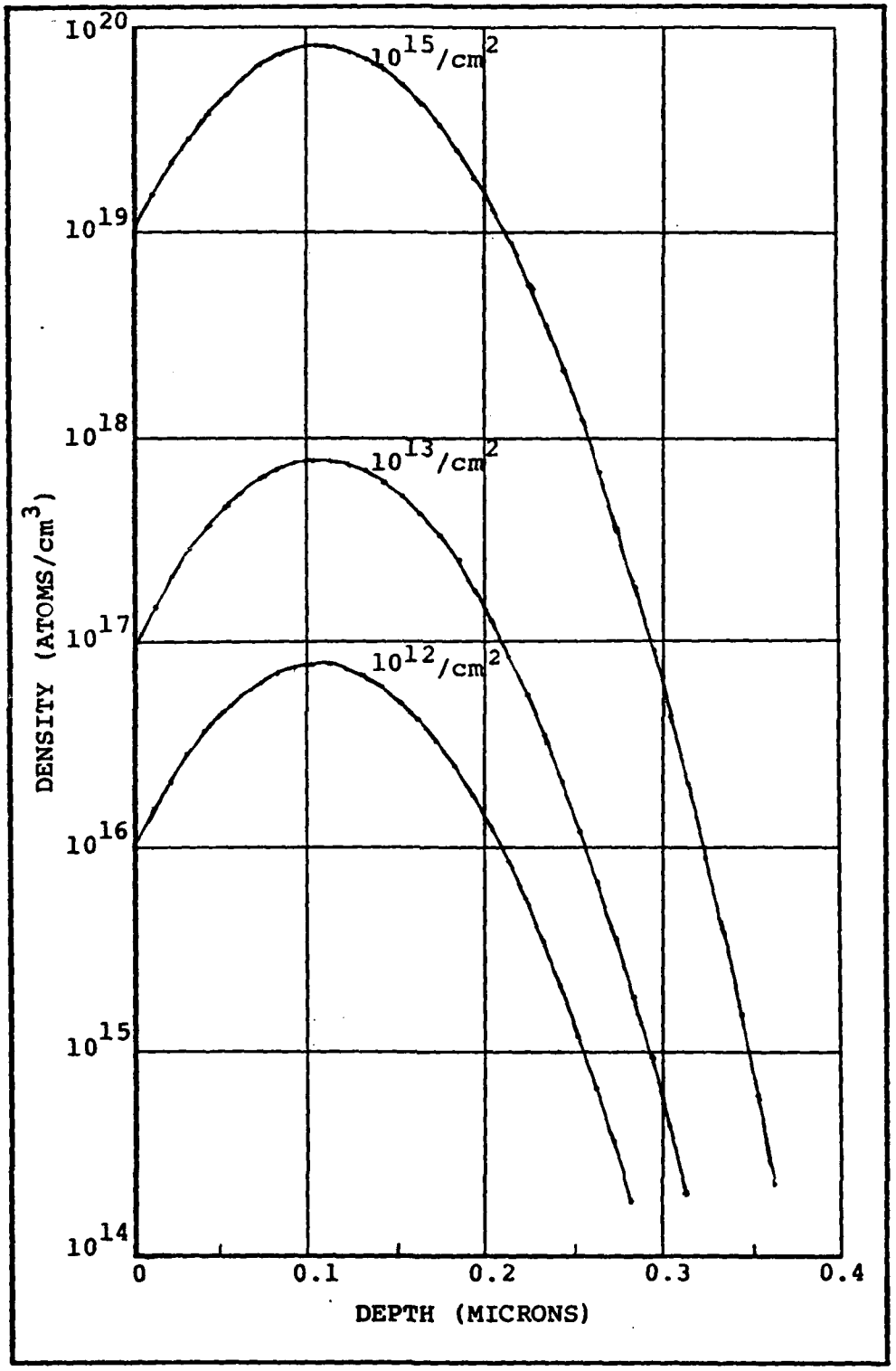

Fig. 2. Concentration of 120 keV Si into GaAs

Fig. 2 have a Gaussian type peak at 1025 Å with a standard deviation of 510 Å. Readers who desire further information on this theory are referred to a detailed work by Gibbons (Ref 14).

In the course of colliding with the lattice atoms, the ions knock some of these atoms out of place creating vacancies and other lattice defects. In addition, the displaced atoms themselves become projectiles and displace even more atoms. The result of all this is the production of an area of damage surrounding the path of the ion. The exact type of damage produced depends on several factors, one being the mass and energy of the incident atom (Ref 24:627). A theoretical damage profile of 120 keV silicon ions implanted in amorphous germanium (Fig. 3) was calculated by AFWAL/AADR from a simple Monte Carlo type computer code. Because of the limitations of the code, the amorphous germanium was used to approximate crystalline GaAs. The definition of "damage" in this code is the amount of energy transferred from the implant ions through collisions. The relative damage is simply the ratio of the energy transferred at any depth to the maximum energy transferred of all depths. As such Fig. 3 only provides a qualitative idea of what the damage looks like. For the purpose of this study, the theoretical damage profile was assumed to follow closely the LSS profiles (Fig. 2). Other studies (Refs 12:848; 25:5765; 2:405), using GaAs samples implanted with various species (mostly Zn and Cd) found that defects were present on the order of 1 μm farther into the crystal than predicted. In a prior thesis, Key (Ref 13) found that damage affected the intensity of the 1.49 eV peak of GaAs as far as 3200 Å - 4000 Å into samples which were identical to those used in the present study.

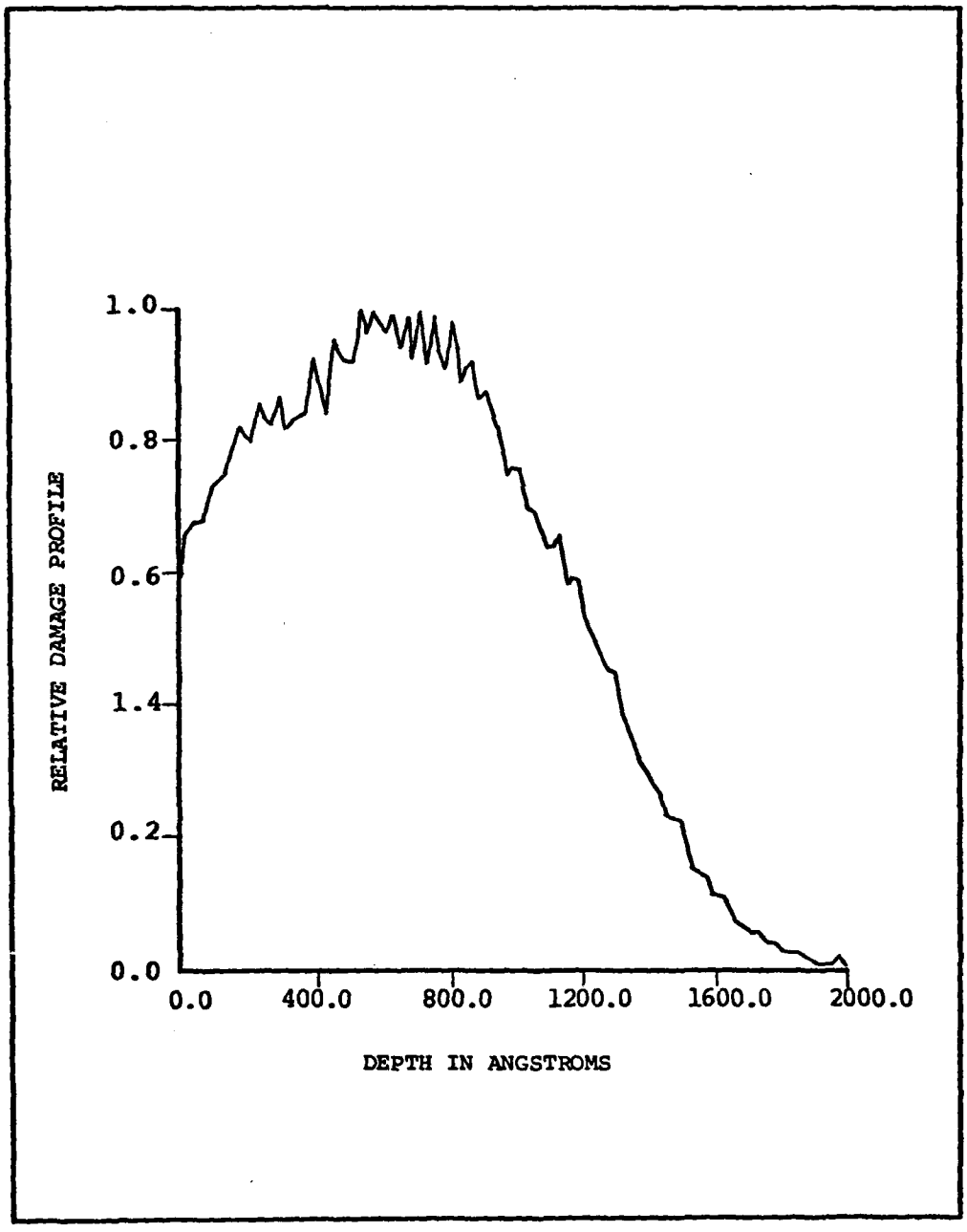

Fig. 3. Theoretical Damage Profile of 120 keV Si into Amorphous Ge

The presence of implant damage in GaAs has been found to reduce luminescent intensity for some types of transitions (Refs 12; 24; 25). This is believed to occur because of additional non-radiative recombination mechanisms being introduced. When the implanted samples are annealed, however, luminescent intensities have been reported to increase due to activation of the implanted ions (Ref 21). Unfortunately, annealing GaAs has some disadvantages (Ref 7:568). Some of these disadvantages involve:

1) depletion of arsenic from the surface starting around 650°C if the surface is not properly capped
2) diffusion of defects and implant impurities into the crystal. This has the effect of flattening out and widening the implant and damage profiles
3) incomplete removal of the damage by annealing at the temperatures available. The surface of the sample will generally have the most damage removed with the effects of annealing dying off in as little as 1000 Å into the crystal (Ref 21).

Because of these disadvantages, determining the damage profile by studying luminescence in annealed samples could be confused by the simultaneous increase of intensity due to activation and decrease of intensity due to residual damage. However several studies, including a prior thesis by Maclin (Ref 21), have reported the prescence of new broad peaks at 1.36 eV and 1.44 eV after annealing. These peaks are not observed in the spectrum of annealed virgin GaAs. In the present study, only data from unannealed samples was used to determine the damage profile.

Laser Penetration

In order to fully understand what regions of the crystal are being excited, it is necessary to know how far into the crystal the excitation source penetrates. For a laser source the intensity of light that is present as a function of depth, x, into the crystal is given by Beer's law:

$$I(x) = I(0)e^{-\alpha x} \tag{4}$$

where

I(x) = intensity of the light as a function of distance into the sample

I(0) = intensity of the light at x=0

e = base of the natural logarithm

α = the absorption coefficient of the material at the wavelength of interest

For a 15mW He-Ne laser at a wavelength of 6328 Å, the absorption coefficient of GaAs is 3.7×10^{-4} cm^{-1} (Ref 29:772). Use of Beer's law with these values yields the distance of one mean free path [I(x) = 1/e of the initial value], defined as the penetration depth, to be 2700 Å. Because of the exponential attenuation of the laser beam with depth, it follows that the greatest amount of absorption occurs at the surface.

Electron Beam Penetration

Since electrons are charged particles their penetration cannot be modeled by Beer's law. The penetration of the electrons into the sample occurs much the same as the penetration of ions during ion

implantation. In this case, however, the electrons are mostly colliding with other electrons in the lattice. As with the ions, the electrons exhibit a depth penetration profile which is Gaussian. However, the statistics of electron depth penetration are more easily modeled if one considers only electron-electron interactions.

Studies utilizing electron beam energies in the range of those used in the present work (E = 1 keV) are not common. Feldman (Ref 11) worked with electron beam energies in this range. Using data obtained at normal incidence with various materials (mostly metals), he modeled his results with an equation of the form:

$$R = bE^r \tag{5}$$

where

R = the penetration depth of the electrons (the peak of the profile)

E = the energy of the electrons in keV

and

b and r are constants related to the material being bombarded

Martinelli and Wang (Ref 22) studied the penetration into GaAs of electrons with energies in the range of 3-7 keV and also fit their results to equation (5). Their values for the constants b and r were respectively, 270 Å and 1.46. Substituting these values into (5) along with the electron beam energy of 1 keV yields a depth of penetration of 270 Å at normal incidence. Since total penetration depths at 45° incidence angle are within 10% of those at normal incidence (Ref 25:3209), the approximation can be made that the penetration depth at 45° is equal to that at normal incidence. This approximation results in a worst case estimate since electrons at normal incidence would be

expected to penetrate farther into the sample than at any other angle. Additionally, it should be noted that the point of greatest excitation will also shift nearer to the surface at 45° incidence.

III. Experimental

The equipment and procedures needed to fulfill the objective of this study are discussed in the following chapter. The order of presentation is: Sample Information, System Setup, Sample Environment, Excitation Sources, Optical System, Optical Alignment, Signal Processing, Cryogenic Transfer, and Etching Procedures.

Sample Information

The GaAs samples used in this study were all high-purity, semi-insulating bulk material grown by the Liquid-Encapsulated Czochralski (LEC) method. Each sample measured 5 mm by 5 mm. Prior to implantation the surface of the samples had been etched in an effort to remove the damage caused by the chemo-mechanical polishing by the manufacturer. This was thought to lie within 15 μm of the surface. Unfortunately, it was discovered too late that only 6 μm were etched off. However, Key (Ref 17) concluded from his data that the 6 μm etched off were sufficient to eliminate the effects of this polishing damage.

The samples were then implanted with 120 keV silicon ions at dosages of 10^{12}, 10^{13}, 10^{14}, and 10^{15} cm^{-2}. Although some of the samples were annealed, all those used in this study were unannealed. Also, because of prior thesis studies no samples of the 10^{14} cm^{-2} unannealed GaAs were available for this study. A spark source mass spectrographic analysis of the virgin GaAs was performed by Wright State University, Dayton, Ohio for AFWAL/AADR. The major impurities were found to be silicon and carbon. The results of this analysis are summarized in Table 2.

TABLE 2

SPARK SOURCE MASS SPECTROGRAPHIC ANALYSIS
OF VIRGIN GaAs (PPM)

Element	ppm
Si	.3
C	.1
Se	<.2
Mn	<.02
Cr	<.02
B	<.03
Al	<.03
Mg	<.03
Fe	<.03
Cu	<.03
Zn	<.04
Ni	<.05
S	<.05

System Setup

The basic system setup is illustrated in Figure 4. The samples were housed in an evacuated cell measuring 15 cm x 15 cm x 15 cm having an access port in each face. The cell was evacuated through the left and bottom port by a Welch Scientific Series 3102D turbo-molecular pump. The back port housed an electron gun used for cathodoluminescence measurements. The front and right ports housed 6.5 cm diameter quartz

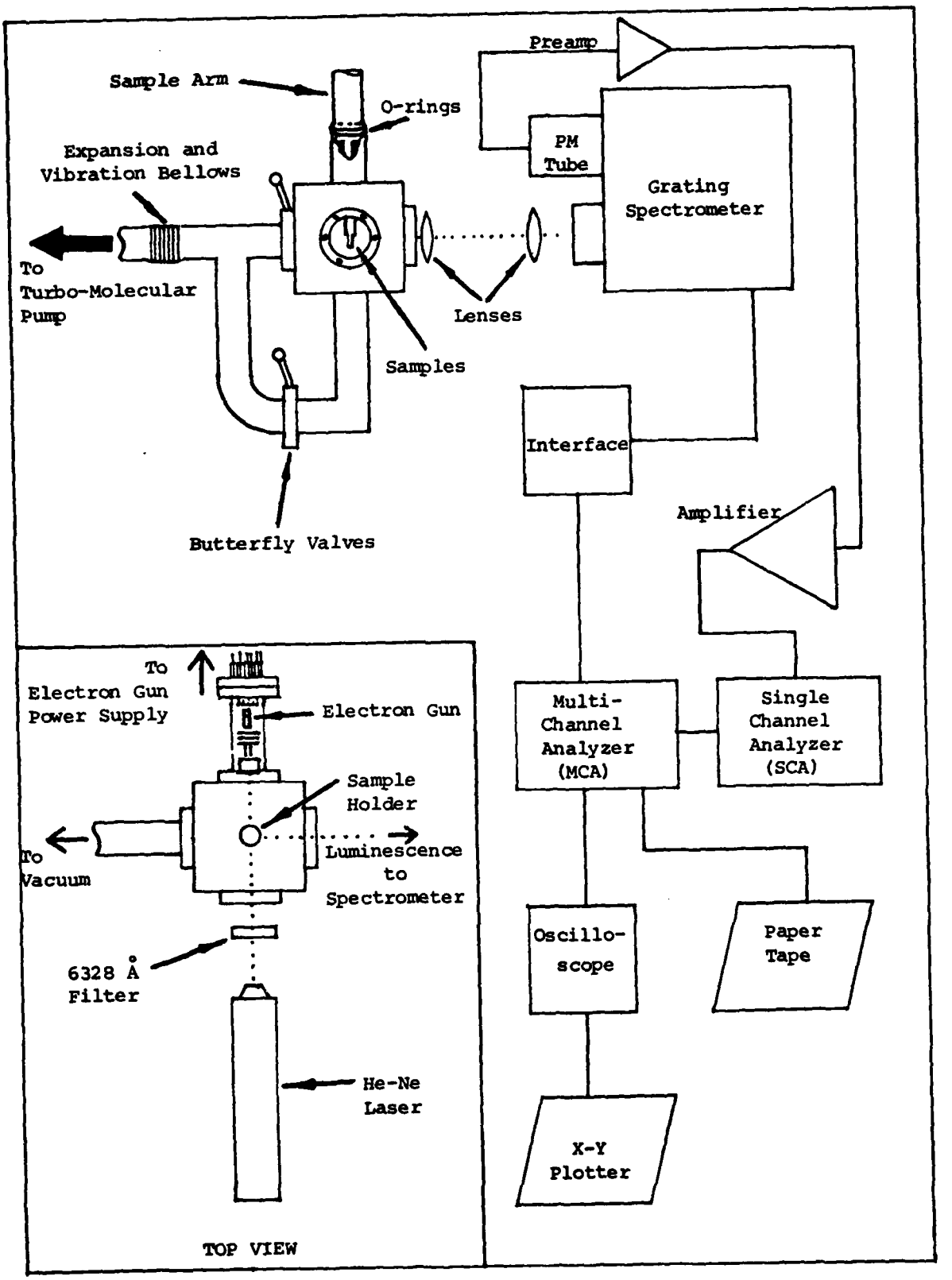

Fig. 4. Experimental Setup

windows. The front window allowed the entrance of the He-Ne laser beam used in the photoluminescence measurements. The right window allowed the luminescence from the samples to exit the cell. The top port consisted of a two inch tube through which the sample arm was placed. The samples were held in place at the end of the sample arm so that they were level with the access ports. The luminescence from the samples was directed through the right window and focused into a grating spectrometer, then detected by liquid nitrogen cooled photomultiplier (PM) tube. The signal from the PM tube was amplified and sent through a discriminator before being recorded by a Multichannel Analyzing System (MCA) where it was displayed on an oscilloscope. The data could then be transferred to an external tape punch or X-Y plotter.

Sample Environment

The cell that the samples were housed in was evacuated using the turbo-molecular pump. Typically the vacuum was maintained between $2x10^{-7}$ torr and $2x10^{-8}$ torr. A Varian ionization gauge located in the back of the pump was connected to a Granville Phillips ionization gauge controller capable of reading down to 10^{-10} torr. The samples being examined were mounted on a copper block (sample holder) at the end of the sample arm (Figure 5A). The samples were held in place by a copper mask bolted to the sample holder with four screws (Figure 5B). The copper mask contained four holes, each 4.5 mm in diameter, to allow for four samples at a time to be examined. Since the width of the laser beam was approximately 2 mm (Gaussian profile) the sample hole size did not interfere with the amount of sample area excited. The electron beam width could be controlled and generally was not larger than 1 mm.

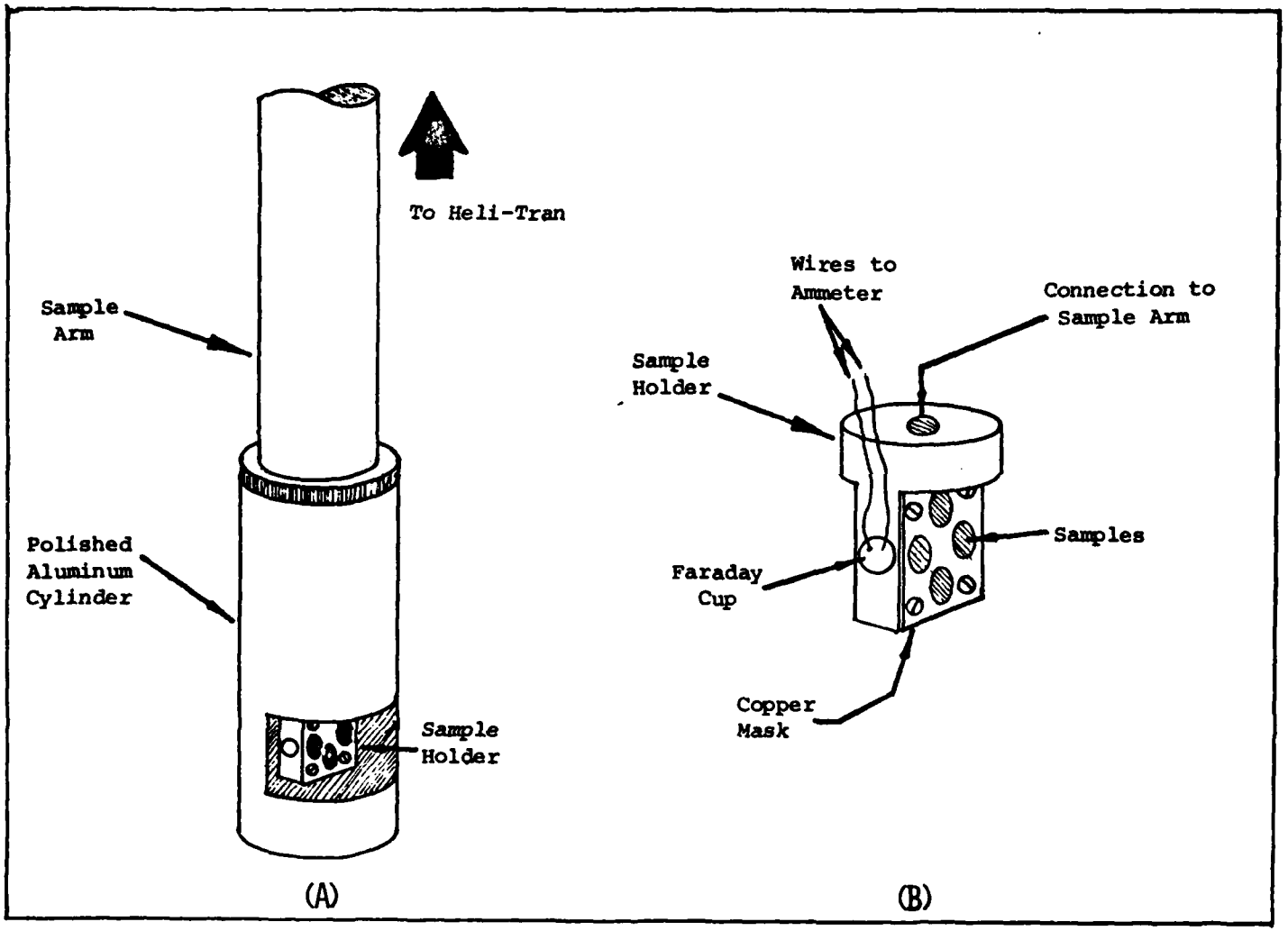

Fig. 5. (A) Sample Arm and (B) Sample Holder

The end of the sample arm and the sample holder were surrounded by a polished aluminum cylinder to minimize the amount of excess energy reaching the samples from the other access ports. A rectangular window was cut out of the side of this cylinder to allow access to the samples by the excitation sources. With the sample arm in place the vacuum was sealed off by two rubber O-rings mounted in a series on the arm. With no other constraints, the arm was easily removed from the cell when there was no vacuum. Additionally, the O-rings allowed the arm and position of the samples to be easily rotated when a vacuum was present. This allowed the samples to be rotated to approximately a 45° angle to either excitation source. Wrapped around the sample arm was a Gold-Chromel thermocouple connected to an Instrulab series 5000 digital thermometer. Also attached to the arm was a resistance heater used to control the temperature of the sample arm via a Lake Shore Cryotonics model DTC 500 cryogenics temperature controller.

Excitation Sources

Laser. The laser used for photoluminescence was a Spectra Physics model 124A 15 mW He-Ne laser. The laser was mounted on two heavy duty ring stands held down with 50 lb. lead bricks. The beam from the laser was aimed directly into the sample cell. A 6328 Å bandpass filter with an 88 Å window had to be placed in the path of the laser beam to minimize the background He-Ne radiation reaching the samples. An attempt was made to expand the beam in order to excite the samples evenly. This idea had to be abandoned when the power density of the laser beam was reduced too much for luminescence to be detected.

This proved not to be a problem, however, since consistent data was obtained from run to run. No estimate was made of the actual power reaching the samples as all the data was relative.

Electron Gun. The electron beam used for cathodoluminescence was produced by a standard RCA electron gun utilizing a barium cathode for the electron source. Figure 6A illustrates the major parts of the gun. Initially, the gun had to be "aged" to rid the cathode of barium oxide. This was accomplished using three different power supplies and applying voltages to the gun as in Table 3.

TABLE 3

AGING OF BARIUM CATHODE ELECTRON GUNS

Time	Filament Voltage	Grid Voltage	Focus Voltage
1 min	6.3	0	0
1.5 min	12.5	0	0
10 min	9.0	+5.0	+150
15 min	9.0	0	0
5 min	6.3	0	0

Occasionally, after the sample cell had been opened, the gun had to be "reaged". The procedure for doing this involved applying a voltage to the filament of 9.0 V, 12.5 V, and 9.0 V for a minute each. This always restored the current from the gun to its original value. During operation the cathode, grid, and filament were typically floated at a -1000 V potential using a Keithley model 240 power supply. The focus

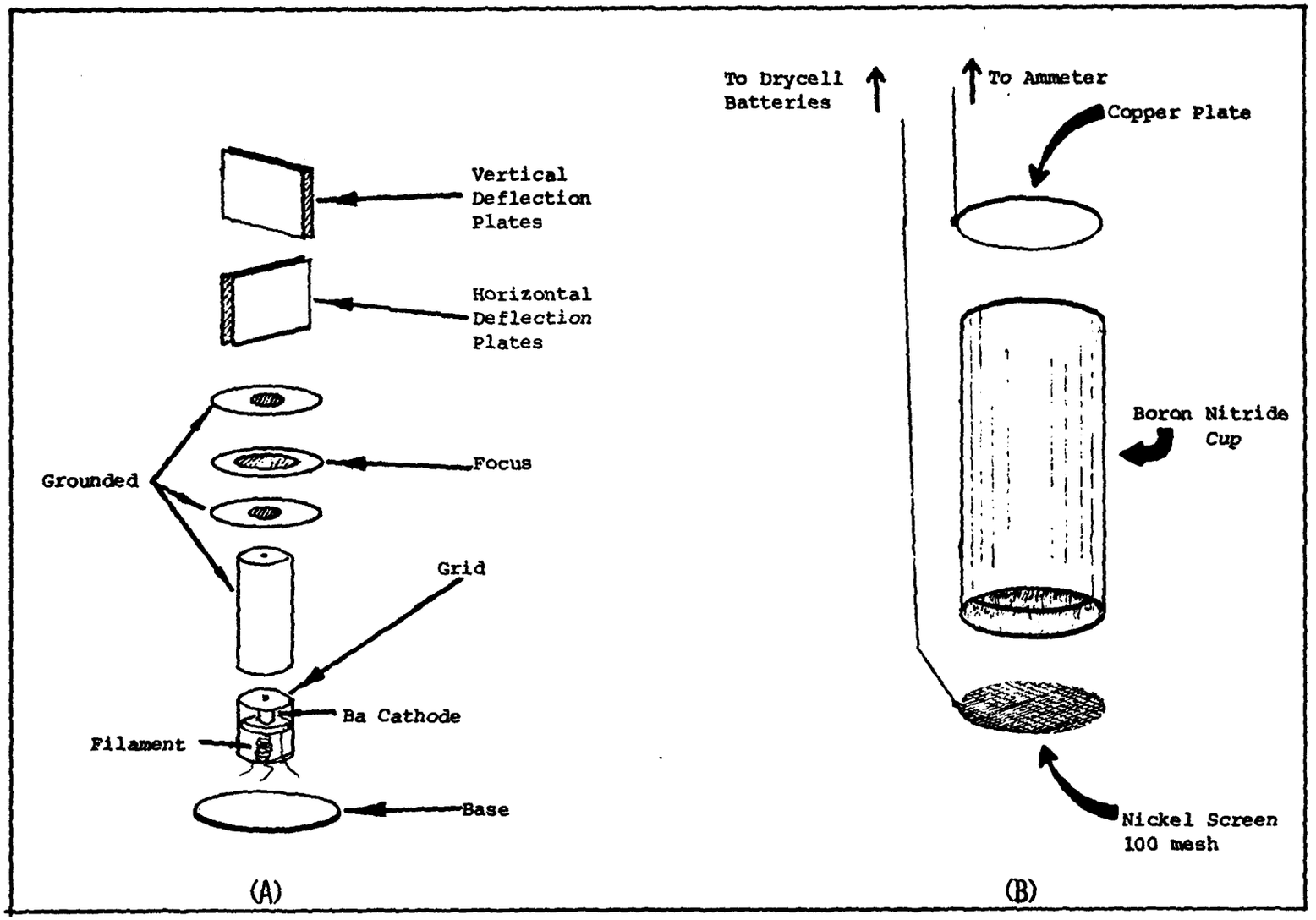

Fig. 6. Major Components of (A) Electron Gun and (B) Faraday Cup

grid was floated around -800 V. The other components were kept at normal ground. The voltage for the deflection plates was provided by three 45 volt drycell batteries grounded in the center of the second battery. This provided approximately ±65 volts to the deflection plates. At a -1000 V potential, the maximum current available from the gun was around 8μA. Most of the cathodoluminescence data was obtained using a current of 5.0 μA.

The currents from the electron gun were measured with a Faraday cup mounted in the side of the sample holder (Figure 5B). The construction of this cup is shown in Figure 6B. The charge collected by the back copper plate was measured with a Keithley model 410 Micro-Microammeter capable of reading currents as low as 10^{-13} amps. The sample arm and beam position had to be adjusted each time the electron beam current was measured.

Optical System

The optical system consisted of two 3.5 cm quartz lenses set up to focus the luminescence from the samples onto the entrance slit of a spectrometer and to slightly overfill the back mirror of the spectrometer (Figure 7). The first lens was located approximately one focal length, 7.5 cm, from the samples. The actual distance varied slightly depending on which opening in the sample mask was being viewed. This lens served to collimate the luminescence being collected. The second lens was placed one focal length, 15 cm, from the entrance slit of the spectrometer. The actual distance of this lens was fine tuned by adjusting the lens' lateral position to focus the image of a center line sample at the slit.

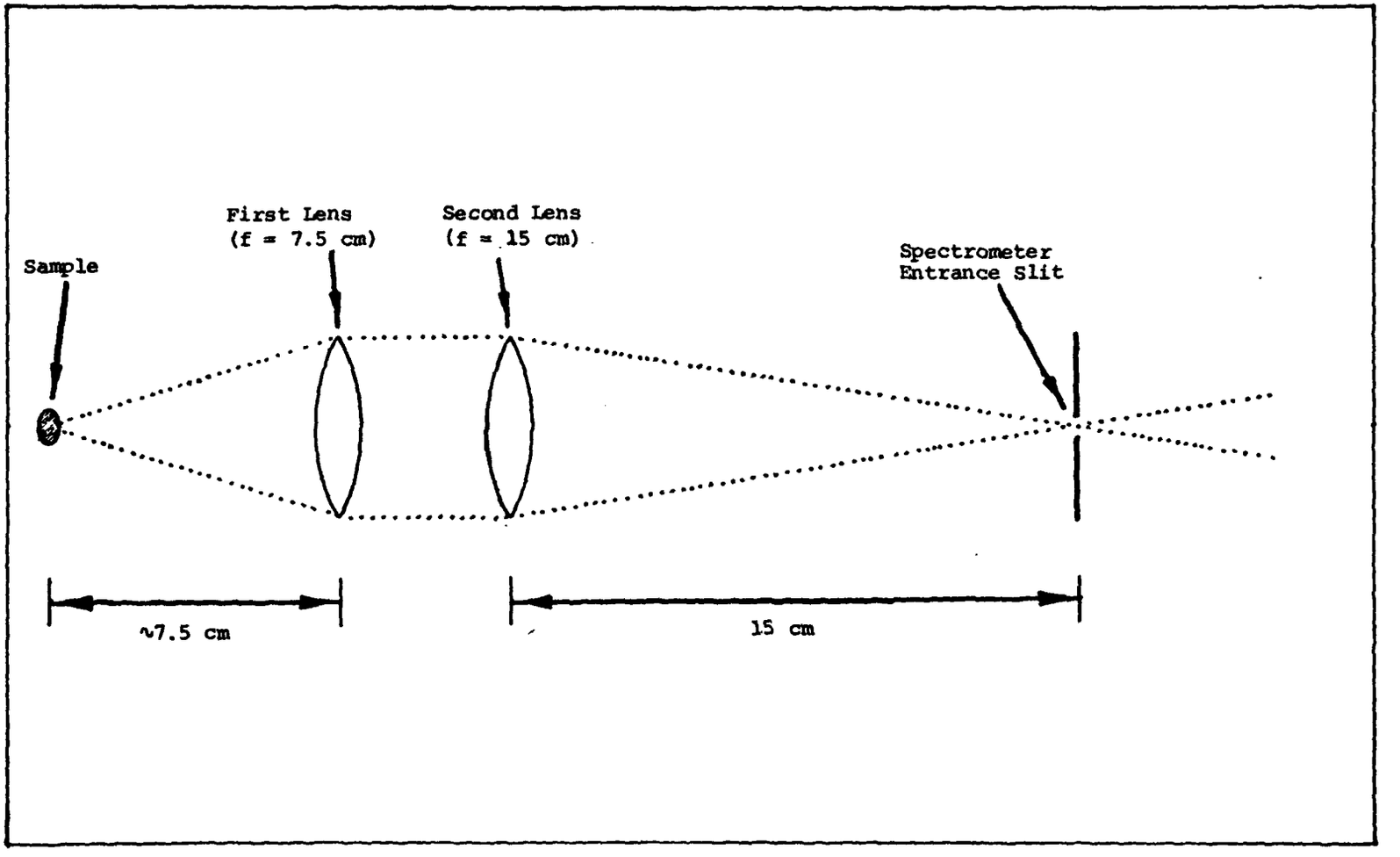

Fig. 7. Lens System Setup

The spectrometer used was a Spex Industries model 1702, three-quarter meter Czerney-Turner scanning spectrometer utilizing a Bausch & Lomb 1200 lines/mm diffraction grating blazed at 5000 Å. The entrance and exit slits were adjustable from 5 μm to 4 mm. All spectra recorded for this study were made with both slits set at 1.0 mm and maximum slit height. The size of these settings was the limiting factor in the resolution of individual lines. Using the tables given in the Spex operating manual the calculated resolution was ±.0009 eV at 1.49 eV.

The light leaving through the exit slit of the spectrometer was collected by a liquid N_2 cooled EMI 9808B photomultiplier tube. This PM tube has an S-1 type cathode and 14 beryllium-copper, linear focus dynodes. This type of tube is sensitive in the 3000 Å to 11000 Å range. A Products for Research model TE 114 photomultiplier tube housing was used to cool the PM tube down to -60°C with liquid nitrogen. The temperature was maintained by a Products for Research model TE 114 control unit. The cathode voltage, which was set at -2000 V, was supplied by a John Fluke model 404M high voltage power supply. Typical dark counts of the PM tube at these parameters were on the order of 100 counts/channel when a scan rate of 57.6 channels/minute was used.

Optical Alignment

The method used for aligning the optics for each run varied depending on which excitation source was used and which sample was being examined. For the laser source, the laser beam was placed on the sample being viewed. The first lens was then adjusted horizontally and vertically so that the sample image was directed into the second lens. With the spectrometer set to the 1.49 eV (8316 Å) luminescence peak in GaAs, the second lens was adjusted to maximize the signal at the MCA.

The first lens was then readjusted and so on until no further adjustment was necessary. When the 1.49 eV peak was too weak to be detected (as in the 10^{15} cm^{-2} sample) a modified procedure was used. The first lens was adjusted as before. However, when adjusting the second lens, instead of maximizing the MCA signal the sample image was simply directed into the entrance slit of the spectrometer. The first lens was then readjusted and the process repeated.

When using the electron gun the same methods could not be used since the electron beam did not produce a visible image of the sample. A Spectra Physics model 142P 2 mW He-Ne laser was incorporated as an aid in aligning the optics for the cathodoluminescence. With this laser, a weak image of the sample could be seen and the procedures discussed above could be followed. Additionally, the laser beam could be aimed directly above and below the sample onto the copper mask. This produced a very bright spot which was used in adjusting the horizontal and vertical positions of the lenses respectively. Once the optics had been aligned using the 2 mW laser, the electron beam was directed onto sample at the same point where the laser beam had been. If the 1.49 eV peak was strong enough to be detected by cathodoluminescence then the deflection and focus of the electron beam were adjusted until the MCA signal was maximized. If the 1.49 eV peak was too weak, then the electron beam was simply placed where the laser beam had been. The position of the electron beam (visible by a faint blue spot) was then checked by placing the laser beam at the same point and reanalyzing the lens position.

Signal Processing

The pulses coming out of the photomultiplier tube were first sent through a Keithley model 104 wide band preamplifier which provided a gain of about 100. From the preamplifier, the signal went through a Tennelec model TC 200 amplifier and then through a Tennelec model TE 411 single channel analyzer (SCA). The SCA helped to filter out spurious low voltage noise pulses which otherwise would be counted. The SCA output was sent to a Hewlett-Packard series 5400A multichannel analyzer (MCA) capable of storing 1024 data points.

The rate that the MCA advanced through all 1024 channels was controlled through a locally built stepper/controller box. This interface box provided several different settings through use of voltage dividers. The interface box was also connected to the stepper motor in the spectrometer so that a precise ratio of Angstroms per channel could be obtained when scanning a range of wavelengths. For the photoluminescence, the spectra were scanned between 8000 Å and 9777 Å in approximately 17 minutes. This gave a ratio of 1.735 Å/channel. The cathodoluminescence spectra were scanned between 8000 Å and 8888 Å in about 20 minutes which gave a ratio of .8681 Å/channel.

The data stored in the MCA was temporarily displayed on an oscilloscope. For permanent storage, the data could be transferred to a paper tape or plotted on an X-Y plotter.

Cryogenic Transfer

The cooling down of the samples was accomplished using an Air Products and Chemicals model LT-3-110 Liquid Transfer Heli-Tran (Figure 8). The heart of this system is a transfer hose which consists of a center transfer tube, the tip flow, surrounded by two interconnected transfer jackets, the shield flow, all enclosed by a vacuum. Liquid helium is

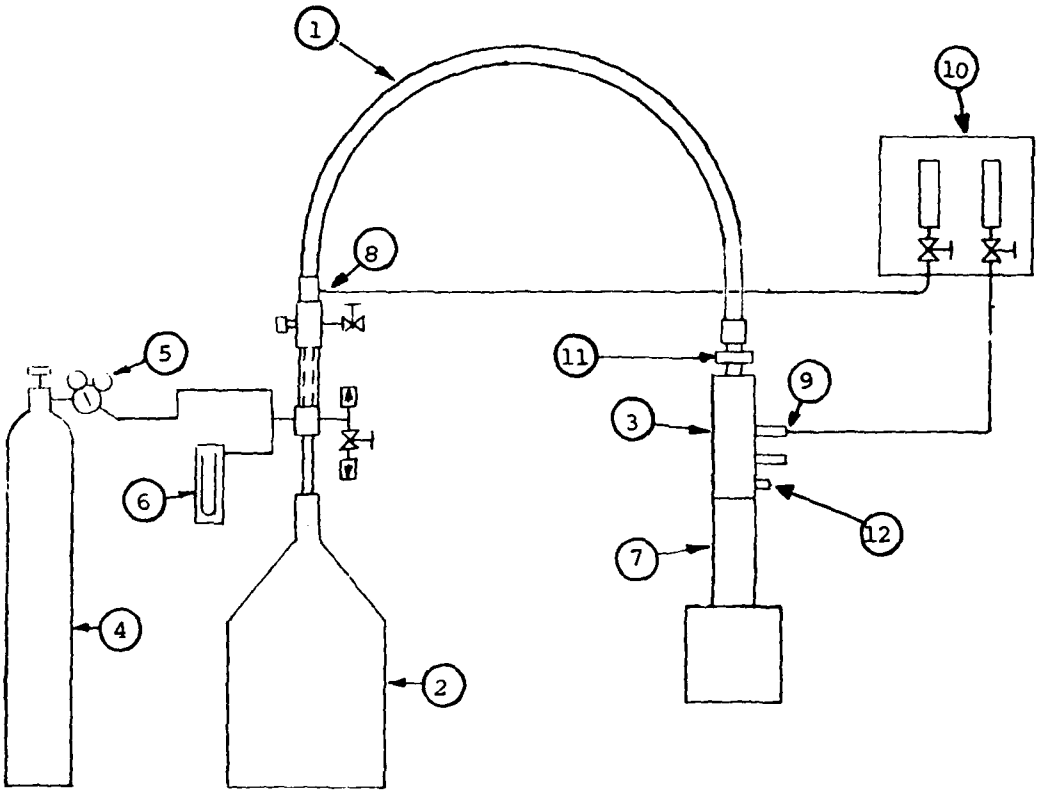

1. Helium Transfer Hose
2. Liquid Helium Dewar
3. Heli-Tran Cold End (Sample Arm)
4. Gaseous Helium Cylinder
5. Pressure Regulator
6. Pressure Gauge on Helium Dewar
7. Sample Cell Inlet Tube
8. Shield Flow Vent
9. Tip Flow Vent
10. Accessory Flow Control Panel
11. Micrometer Valve Adjustment
12. Transfer Hose Evacuation Port

Fig. 8. Heli-Tran Setup

drawn out of a helium dewar into the tip flow and shield flow by applying a positive pressure. The helium in the tip flow travels through the transfer hose to the sample holder and exits just above the sample arm. The helium in the shield flow travels to the sample arm in an inside jacket, then backtracks in an outside jacket to the dewar where it is vented. The helium exiting from the two flows is diverted to two flow control valves which are used to control each individual flow. In addition to these, the flow of helium through the tip flow can be controlled by a needle valve located in the sample arm. The temperature of the sample holder was measured via a Gold-Chromel thermocouple wrapped around the arm. Typically, a sample temperature of 7° - 8° K was obtained. External to the helium transfer system was a cryogenic resistance heater for controlling the temperature. Because this heater was unstable at such low temperatures, it was only used to speed up warming the arm at the end of a run.

The procedure for cooling down the samples was as follows. With the two flow control valves wide open, the end of the helium transfer hose was partially inserted into the helium dewar. Gaseous helium was then drawn through the entire system to purge any water vapor. After about fifteen minutes, the hose was lowered all the way into the dewar to start the liquid helium flowing. If the transfer hose had previously been inserted in the dewar (from a prior run) then it was not necessary to purge the system with gaseous helium. The internal pressure of the dewar was adjusted and kept around 5 psi. Generally, the sample arm cooled down completely in an hour. Once the samples had been cooled down, the flow of helium was adjusted as described in the Heli-Tran operating manual in order to minimize

helium usage but still maintain stability and temperature. As a rule, the system vacuum was allowed to reach $2x10^{-7}$ torr before cooldown was started. This was done to minimize the amount of impurities solidifying out on the sample surfaces.

When a run was finished it was necessary to warm the system to room temperature before removing the sample arm from the cell. The procedure for this involved closing the flow control valves to stop the helium flow and allowing the system to warm up on its own. When a fast warm up was needed, the cryogenic heater was used. This reduced the warm up time from a normal 2 hours to 1 hour.

Etching Procedures

In order to evenly etch off layers of the sample for each run, a chemical etchant was used. This etchant consisted of a solution of sulfuric acid:hydrogen peroxide:water in the proportions of 1 ml:1 ml: 50 ml (Ref 16:768). Two temperatures were used for etching, 3°C and 23°C (room temperature). The 3°C solution was cooled down by surrounding a beaker of the etching solution with an ice bath. The choice of 3°C was simply a matter of convenience in that additional cooling of the solution to approximately 0°C doubled the time required for this step. Table 4 lists the resultant amounts etched off for different etching times and temperatures.

The basic procedure for etching was as follows. The samples were cleaned initially by submerging them successively in solutions of trichloroethylene (TCE), methanol, and acetone for a few minutes each. The cleaning solutions were each suspended in a vibrasonic cleaner filled with water. The samples were then rinsed with 18 meqohm water

TABLE 4

ETCH RATES OF THE ETCHANT
$H_2O_2:H_2SO_4:H_2O$ IN A 1:1:50 RATIO

Temperature	Time (sec)	Amount Etched (Å)
3°C	30	150
3°C	90	500
23°C	50	800

and dried with the edge of a clean Kimwipe. So that the amount of etch could be measured, a reference GaAs sample had half of its surface coated with wax to prevent etching of that area. Following cleaning, 50 ml of 18 meqohm H_2O was measured out with a graduated cylinder and poured into an 80 ml beaker. Using a pipet, 1 ml of 36N (18M) H_2SO_4 was added. At this point, if the etching solution needed to be cooled, the 80 ml beaker was set in an ice bath. The H_2O_2, which was kept refrigerated and in the dark, was not added until the last possible moment to reduce any degradation of the solution during this time. Once the solution was at the right temperature (3°C) 1 ml of 30% H_2O_2 was pipeted into the acid-water solution and the solution was lightly stirred.

To etch, all the samples (including the reference) were submerged in the etching solution simultaneously and a timer started. When the alloted time had ellapsed, the samples were taken out of the etching solution and immediately submerged in a beaker full of 18 meqohm water to stop the reaction. The samples were then cleaned individually as before. The reference sample, after being cleaned, was examined for

etch depth with a Sloan Dektak surface profile machine. Normally, the reference sample was only examined when the etching rate was changed. This was necessary to conserve time and also because the smaller etch rates were close to the sensitivity limits of the Sloan Dektak.

The concentration of the stock peroxide solution was checked periodically for degradation by titration with a thiosulfate solution. At the beginning of this study, the concentration was found to be very close to full strength (30%). Subsequent titrations showed little change in H_2O_2 concentration. The procedure for performing the titration is outlined below (Ref 19:283).

PEROXIDE TITRATION WITH THIOSULFATE

Solutions needed: 4N H_2SO_4

1N KI

.1N Thiosulfate (standardized)

Procedure:

1. Dilute the peroxide solution so that it is ∿.1N (Full strength H_2O_2 is ∿12M)
2. Take a 25 ml aliquot of the dilute H_2O_2 solution.
3. Add 10 ml of 4N H_2SO_4.
4. Add 6 ml of 1N KI.
5. Let the solution set at least 15 minutes. (Ammonium molybdate can be used as a catalyst here).
6. Titrate with standard thiosulfate solution until the solution stays clear at least 30 seconds.

Note: The solution is a dark reddish brown color and gradually clears up at the endpoint. To help distinguish the

endpoint, a few drops of starch indicator should be added just before the endpoint. This results in a dark blue solution which turns to clear.

The thiosulfate solution is not stable more than a few days. Since the materials needed to standardize the thiosulfate solutions were not available, it was necessary to make up new solutions each time a titration was performed. The actual concentration of the thiosulfate solution was therefore always assumed to be equal to its calculated concentration.

IV. Results and Discussion

Luminescence of the Samples

In Chapter 2, it was pointed out that using luminescence data obtained from annealed GaAs to derive the damage profile would be difficult due to:

1) depletion of arsenic from the surface starting around 650°C if the surface is not properly capped
2) diffusion of defects and implant impurities into the crystal
3) incomplete removal of the damage by annealing at the temperatures available

Additionally, the mechanisms causing the peaks which have been observed at 1.37 eV and 1.44 eV in annealed samples are not completely understood. For these reasons and also to supplement the work done by Key (Ref 17) it was decided to concentrate on the unannealed samples and study the annealed samples if time were available. Unfortunately, time did not permit studying the annealed samples.

GaAs samples implanted at four different dosages of silicon ions were used throughout this study. The four dosages were:

1) 10^{15} silicon ions/cm^2
2) 10^{13} silicon ions/cm^2
3) 10^{12} silicon ions/cm^2
4) No dosage - virgin GaAs

The virgin (control) sample was treated in exactly the same manner as the implanted samples. The luminescent intensity from this sample was used to normalize the spectra of the implanted samples.

In both the photoluminescence and cathodoluminescence data only three peaks attributed to GaAs were ever resolved. A typical GaAs spectrum showing these peaks is represented in Figure 9. The first peak was a weak peak located at 1.5117±.0013 eV. This peak was observed in the virgin sample at all etch depths. The location of this peak and its low intensity are consistent with other reports that this peak is due to bound exciton recombination. The bound exciton in this case is thought to be bound to a neutral acceptor (Ref 31:342). This peak was seen occasionally in the 10^{12} ion/cm^2 sample, but was not observed initially in the other samples. Even after etching completely through the damage layer, the intensity of this peak in the implanted samples was lower than that in the virgin GaAs.

The second peak, and the one used for the normalized plots, was located around 1.49 eV. It was apparent in most samples that this peak contained at least two individual peaks. These peaks were not individually resolvable, but their locations could be estimated from the distortions in the shape of the overall peak (Fig. 9). Of the two methods of excitation used,photoluminescence seemed to provide slightly better definition in this peak. Additionally, the ratio of intensities of these two peaks was not constant from run to run. However, the observed deviations followed no order and kept within the statistical fluctuations which might be expected in such counting data. In the majority of the runs, a peak at 1.4904±.0009 eV was more intense. For the rest, a peak at 1.4933±.0009 eV was observed to be prominent. Cross correlation between Tables 1 and 2 leads one to conclude that the peak at 1.4933 eV is due to a band-acceptor transition involving carbon. Also, if in Table 1 the higher value for silicon is referenced,

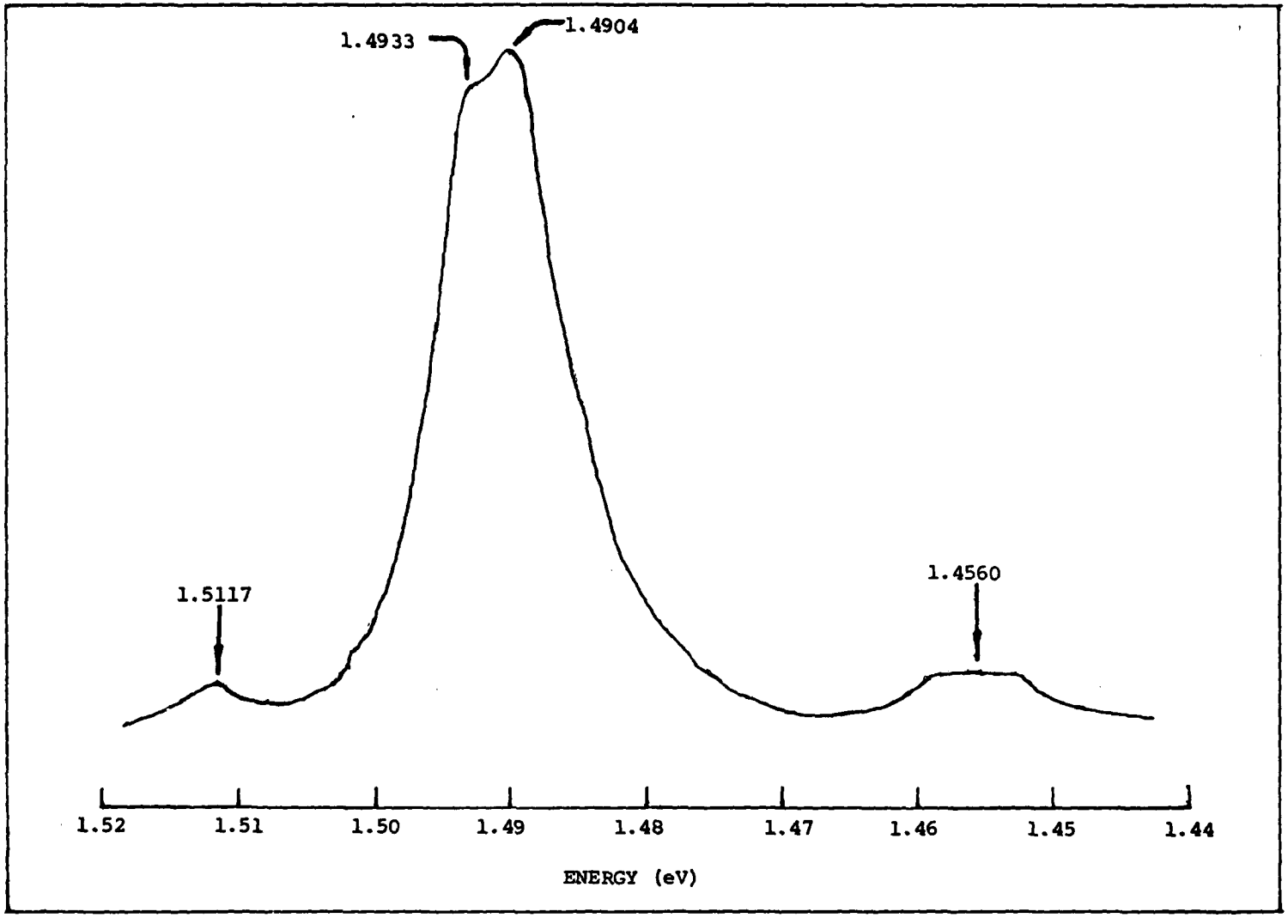

Fig. 9. Typical Spectrum of GaAs Around the 1.49 eV Peak

then the peak at 1.4904 eV can be attributed to a band-acceptor transition involving silicon. Since both of these elements can act as acceptors in GaAs, it seems logical that acceptor peaks associated with them would be present. That this peak had previously been attributed to an acceptor-donor (bound-bound) transition (Ref 17) should be noted. In all samples, the luminescent intensity of the 1.49 eV peak never increased beyond that for the virgin sample. This would indicate that the implanted silicon ions do not contribute to the intensity of this peak. Additional support is given to this conclusion when one remembers that the ratio of carbon to silicon luminescent intensities in the 1.49 eV peak remained relatively constant irregardless of dosage or depth. In other words, the ratio of carbon to silicon ions remained the same.

The third resolved peak that was observed in most of the spectra was located approximately 36 meV lower in energy than the 1.49 eV peak. The difference in energy between these two peaks is very close to the energy of one phonon assist (36 meV). This peak is therefore considered to be a phonon replica of the 1.49 eV peak. The photoluminescence spectrum of this peak did show some definition of other peaks (Fig. 9). The cathodoluminescence spectrum of this peak did not show as much definition, presumably due to the lower excitation intensity.

The data involving peak resolution could have been improved by optimizing system parameters. It should be pointed out, however, that the primary objective of this work was to observe changes in luminescent intensity rather than trying to resolve individual peaks. For this reason, system parameters were adjusted to increase the intensity, which out of necessity will tend to degrade resolution.

Depth Resolved Profiles

Photoluminescence. Photoluminescence spectra from the surface of the four GaAs samples are presented in the Appendix. In the virgin sample the intensity of the 1.49 eV peak appeared to increase about 7% within a few hundred angstroms of the surface. Although this is not a significant amount, it might indicate a larger presence of non-radiative recombination mechanisms nearer the surface. The intensity of this peak was also observed to increase about 20% in cooling the samples from 8°K to 7°K.

In the luminescence spectra of the implanted samples, no new peaks were observed. Initially, the three resolved peaks were either nonexistent or much lower in intensity than those of the virgin sample. Also, the position of the two lines making up the 1.49 eV peak did not show any shift in energy as a function of dosage.

A plot of the normalized photoluminescent intensity of the 1.49 eV peak as a function of etch depth is shown in Figure 10. As can be seen from this figure, the 1.49 eV peak was present initially in both the 10^{12} and 10^{13} ions/cm^2 spectra but not in the 10^{15} ions/cm^2 spectrum. The 10^{15} ions/cm^2 spectrum started showing this peak at 450 Å. After initial detection, relative peak intensities for all implanted samples were seen to steadily rise as etch depth increased. A leveling off of the normalized intensities is apparent as these values approach 1. This would be expected if a Gaussian damage profile were present. The fact that no luminescence is seen in the 10^{15} ion/cm^2 spectrum initially indicates that this sample contained a "dead" layer (<.01 normalized intensity) where luminescence was completely quenched. Consideration of this with the penetration depth of the laser would

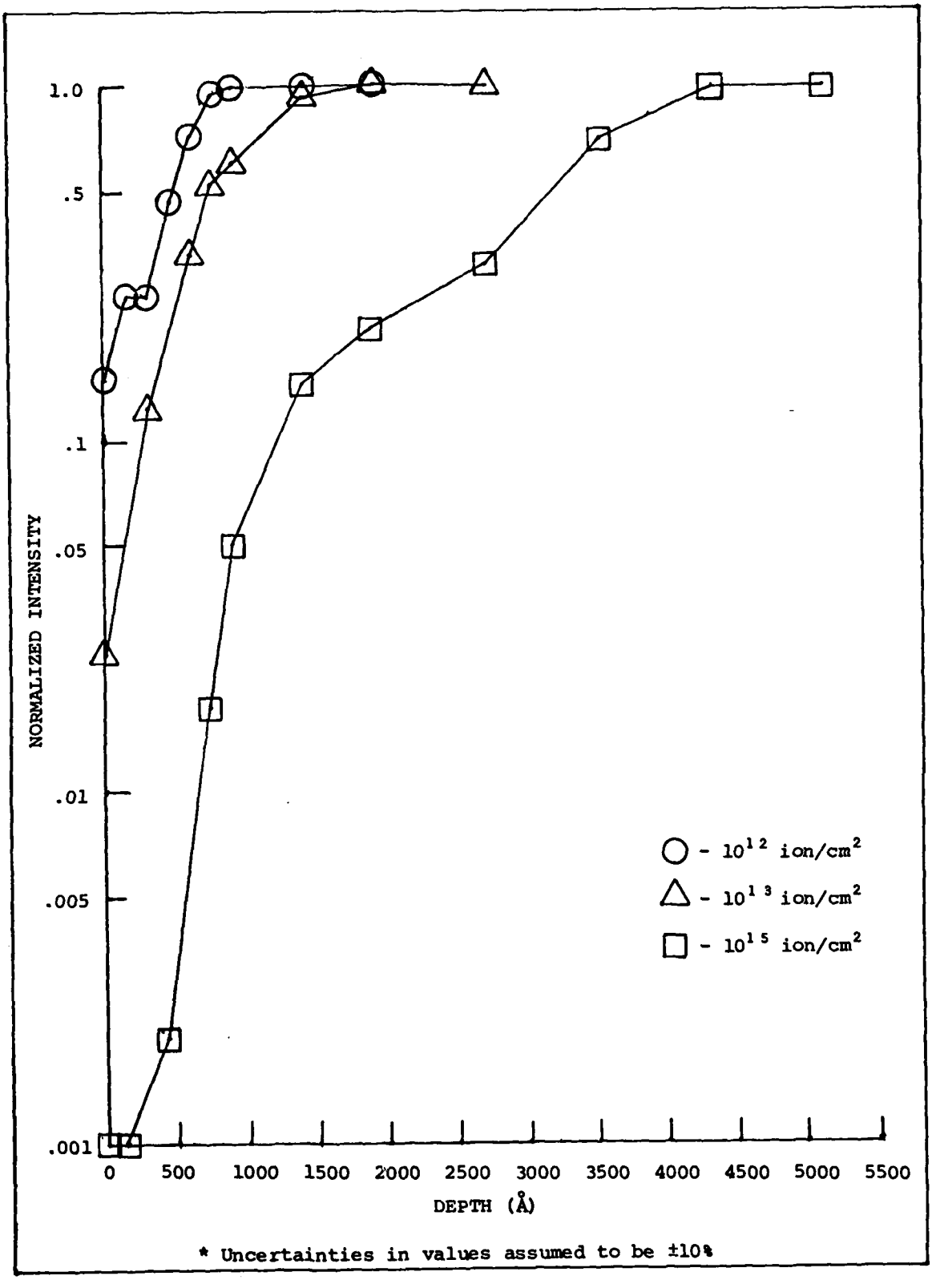

Fig. 10. Normalized Photoluminescent Intensities

make the dead layer roughly 3100 Å deep (2700 Å + 450 Å). Correspondingly shallower depths would be present for lower dosages. This latter statement is supported by examining the low normalized intensities of the other 10^{12} and 10^{13} ion/cm^2 samples. Contrary to the findings of Key (Ref 17), no dip in the plot of normalized intensity around 800 Å was seen for any of the samples. This is most likely a result of differences in penetration depths. Key's excitation source was an argon laser which only penetrated about 1000 Å into the sample. If the peak of damage occurs around 1000 Å, then his source had not passed it yet. By contrast, the He-Ne laser used for the present study penetrated 2.5 times farther, well past the peak in the damage profile. This caused the dip in the plot to be disproportionately "averaged" out by luminescence from deeper in the crystal. Tied to this also is the explanation for the normalized intensity for all samples steadily increasing with etch depth.

The depths at which the luminescent intensities were completely restored were consistent with what Key found when one also considers the differences in laser penetration depth, i.e. the depths found in the present study were slightly shorter than those of Key. The restoring depths were respectively from lowest dose to highest 900 Å, 1900 Å, and 4300 Å.

Cathodoluminescence. Surface cathodoluminescence spectra for all four samples are located in the Appendix. A plot of normalized intensity for the cathodoluminescence data is presented in Figure 11. This plot is similar to the one presented for photoluminescence in that no dip in the plot is observed and the normalized intensities are seen to rise steadily. In this case, however, the reason for the absence of the dip

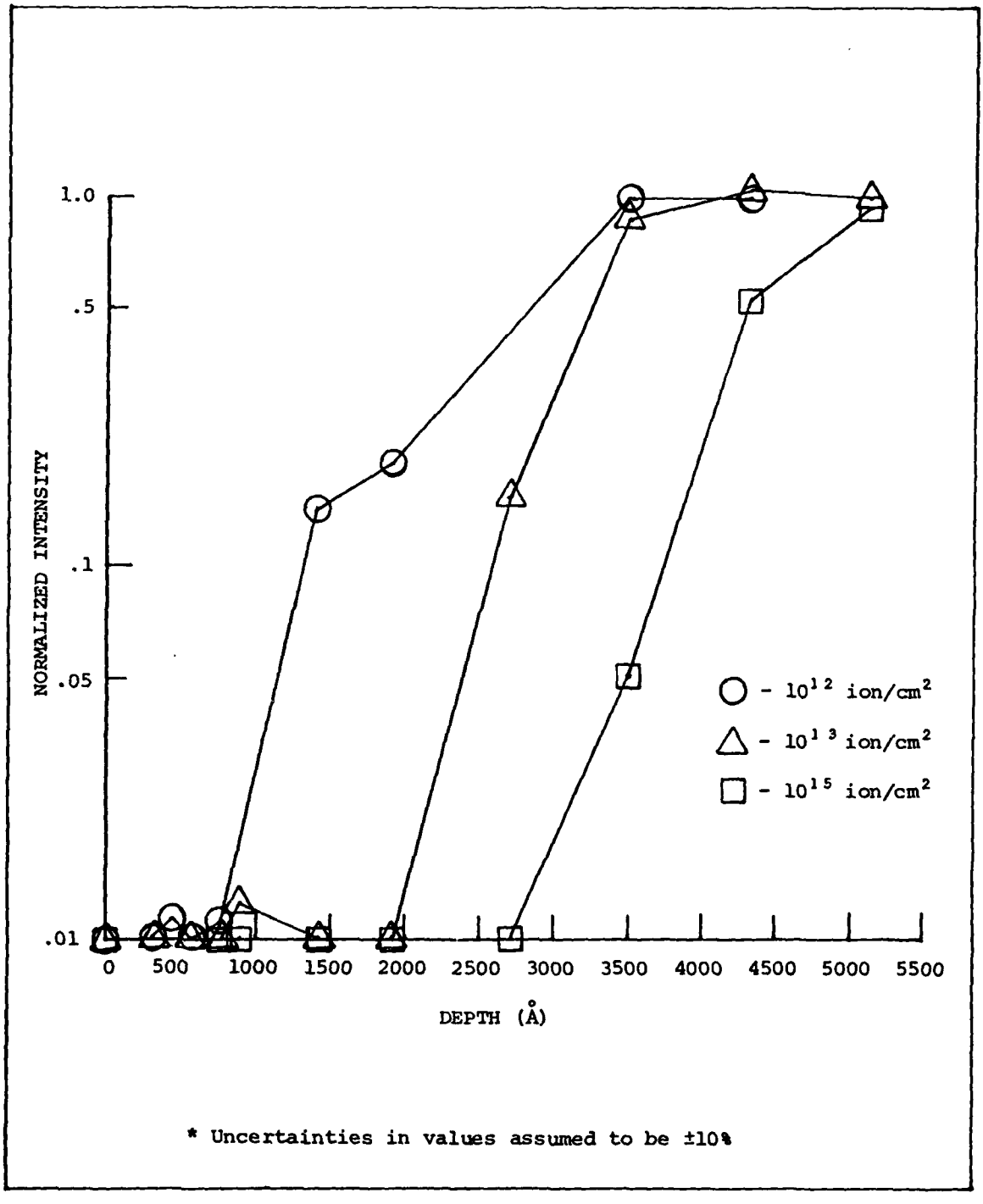

Fig. 11. Normalized Cathodoluminescent Intensities

is not the same. The depth of penetration of the electron beam is short enough (270 Å) that the damage peak will not be "averaged" out. Instead the intensity of the electron beam, and therefore the cathodoluminescence produced, was so low that adequate luminescent intensities were not observed until the peak in the damage profile had been etched away. Even at the surface, where the amount of damage present should be less than that at the damage peak, all luminescence was quenched ($<$.01 normalized intensity). In fact, the most noticeable difference of the cathodoluminescence plot from the photoluminescence plot is that the luminescence from all the implanted samples is initially quenched. A "dead" layer must be present for all implanted samples. According to Fig. 11 this layer extends 1400 Å into the surface for the 10^{12} ion/cm^2 sample and increases to 3500 Å for the 10^{15} ion/cm^2 sample. The presence of the dead layers supports the idea in the photoluminescence section that the initial normalized photoluminescent intensities of the two lower dosage implanted samples were a result of averaging out the dead layer.

It is interesting to note that for the 10^{12} ion/cm^2 sample the size of the dead layer (1400 Å) is close to the peak position in the LSS profiles (1025 Å). If the LSS profiles are considered to be accurate in modeling the damage profiles also, then only a small region surrounding the peak position would be expected to quench luminescence. The concentration of damage at and near the surface would appear from Figure 2 to fall below that required to quench all the luminescence. In reality, all luminescence up to the surface is quenched, even though for the same ion density on the inward side of the profile peak luminescence is observed. Even if one adds in the penetration depth of

the electron beam (270 Å) and extends the dead layer,there still should be some luminescence observed at the surface according to the LSS profiles. This inconsistency is probably a result of one of two things: either the actual damage profile can not be modeled with the LSS profiles or the theory behind the LSS profiles is flawed.

Assuming that the LSS profiles are accurate and that they model the damage profile closely and if one draws a horizontal line on Figure 2 from where the 10^{12} ion/cm^2 curve intersects the dead layer depth (1400 Å in this case), then the depths at which the line crosses each dosage curve can be plotted as a function of dose to predict the depths of initial detection. The validity of this method relies on the assumption that the luminescence always becomes detectable at the same impurity ion concentration. If one then takes a value of 1400 Å for the 10^{12} ion/cm^2 sample and plots the depths obtained, Figure 12 results. On the same plot is the data from actual (experimental) depths of initial detection for each implanted sample. Notice that the experimental depths increase with dosage faster than predicted. If the LSS profiles are accurate, the two sets of data should be very close to each other with about the same rate of increase. Therefore, the discrepancy in Figure 12 leads to one conclusion that some diffusion of defects and/or implanted ions occurred, either from the implant process or thermally at room temperature. However, the previous analysis involving the 10^{12} ion/cm^2 sample dead layer and the results in Figure 12 both support the idea that the LSS profiles are flawed and do not represent the damage and implant profiles accurately. In the case of Figure 12, the assumption that the damage profile is modeled by the LSS profiles closely is not crucial to the above argument. Even if the ranges of each profile are

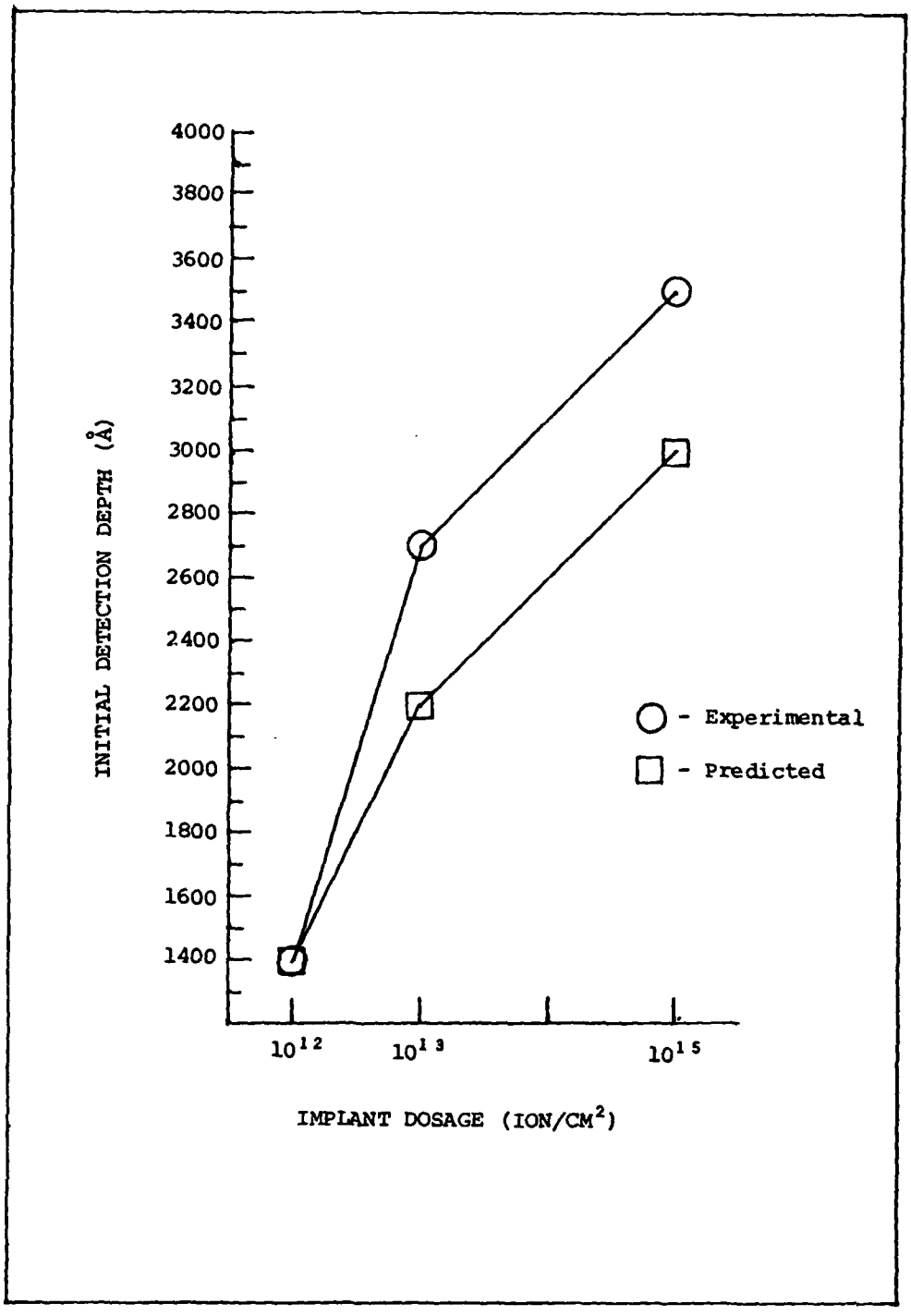

Fig. 12. Comparison of Initial Cathodoluminescence Detection Depths with LSS Profiles

not the same (i.e. different peak ranges), the differences in range with dosage for each profile would be expected to be approximately the same (the damage profile is not likely to greatly outreach or fall behind the implant profile even if the two are not exactly the same curve).

Besides the region of luminescence quenching, the curves in Figure 11 (cathodoluminescence) appear to rise at a steeper rate than those in Figure 10 (photoluminescence). This is logical since the cathodoluminescence data would be expected to more closely model the actual damage profile due to the shorter depth of penetration. Again, some leveling off of the data as unity is approached can be seen. The depths at which the normalized cathodoluminescent intensities became unity were from the lowest dose to the highest respectively 3500 Å, 4300 Å, >5100 Å (the intensity of the 10^{15} ion/cm^2 sample had not been completely restored at the last etch performed but gave a normalized value of .98). These values are much greater than Key found. This is not unreasonable considering the shorter penetration depth of the electron beam.

While making the cathodoluminescence measurements a problem was noticed when carbon deposits formed on the surface where the electron beam was hitting. These deposits were most likely the result of electrons breaking down oil (or other organic matter) into carbon and hydrogen. This deposit could not be cleaned off. Additionally, it was found that these deposits greatly reduced the luminescence collected. The solution to this problem was to always move the electron beam to a new area of the sample. Fortunately, the size of the electron beam was small enough that a new area could always be found. This phenomena has the potential to be a major disagvantage however.

V. Conclusions and Recommendations

Conclusions

The implantation of silicon ions into unannealed GaAs did not produce any new peaks in the range 8000 Å to 9777 Å which was expected. Additionally, the intensity of the native peaks of virgin GaAs were not augmented by the implanted ions. The only effect observed was the increased quenching of the native peaks with increasing dosage. For all three of the implanted samples, a "dead" layer was observed with cathodoluminescence in which luminescence was completely quenched. This layer extended 1100 Å into the surface for the 10^{12} ions/cm^2 sample and up to 3700 Å into the surface for the 10^{15} ions/cm^2 sample. In addition, the intensity of the 1.49 eV peak was affected by damage as far as 5100 Å into the surface, much farther than Key found. No dip in the normalized intensity plot was observed, but instead the normalized intensities were seen to rise steadily as etch depth increased. The data from the cathodoluminescence tended to show a steeper rise in intensity than the data from photoluminescence. Correlation of all the data from cathodoluminescence with the LSS profiles indicated that either some diffusion of defects and/or implant impurities had occurred or that the theory behind the profiles is flawed.

Examination of the 1.49 eV peak in the luminescence spectra of the samples revealed at least two individual peaks. These peaks appeared to be located around 1.4904 eV and 1.4933 eV. They were attributed to band-acceptor transitions involving silicon and carbon respectively.

Recommendations

It is recommended that further studies be performed on similar samples to those used in this study in an effort to observe the peak in the damage profile. Such studies should rely on minimum penetration excitation sources, preferably a UV source, and etch in smaller increments to obtain a smoother profile. An electron gun could be used as the excitation source, but the higher currents needed might enhance the formation of carbon deposits on the surface. It would also be interesting to look at the annealed samples in an attempt to determine the nature of the 1.37 eV and 1.44 eV peaks.

Bibliography

1. Air Force Avionics Laboratory. Technical Programs and Contracts (Tenth Edition). March 1979.

2. Aoki, K., et al. "Depth Distribution of Defects in Mg-Ion and Cd-Ion Implanted GaAs," Japanese Journal of Applied Physics, 15(2):405-406 (February 1976).

3. Ashen, D. J., et al. "The Incorporation and Characterization of Acceptors in Epitaxial GaAs," Journal of Physics and Chemistry and Solids, 36(10):1041-1053 (October 1975).

4. Bebb, H. B., et al. "Photoluminescence I: Theory," Semiconductors and Semimetals, Volume 8, edited by R. W. Willardson and Albert C. Beer. New York: Academic Press, 1972.

5. Bogardus, E.H. and H. B. Bebb. "Bound-Exciton, Free-Exciton, Band Acceptor, Donor Acceptor, and Auger Recombination in GaAs," Physical Review, 176(3):993-1002 (December 1968).

6. Boulet, D. L. Depth Resolved Cathodoluminescence of Cadmium Implanted Gallium Arsenide. Unpublished MS thesis. Wright-Patterson Air Force Base, Ohio: Air Force Institute of Technology, December 1975.

7. Chatterjee, P. K., et al. "Photoluminescence from Be-Implanted GaAs," Applied Physics Letters, 27(10):567-569 (November 1975).

8. Colbaw, K. "Free-to-Bound and Bound-to-Bound Transitions in CdS," Physical Review, 141(2):742-749 (January 1966).

9. Cusano, D. A. "Identification of Laser Transitions in Electron-Beam Pumped GaAs," Applied Physics Letters, 7(6):151-152 (September 1965).

10. Dmitruk, N. L., et al. "Electrophysical and Luminescence Properties of Implanted GaAs," Radiation Effects, 49:51-56 (1980).

11. Feldman, Charles. "Range of 1 - 10 keV Electrons in Solids," Physical Review, 117(2):455-459 (January 1960).

12. Gavrilov, A., et al. "Photoluminescence Investigation of the Distribution of Defects in Gallium Arsenide After Ion Bombardment," Soviet Physics of Semiconductors, 10(8):847-848 (August 1976).

13. Gershenzon, M. "Radiative Recombination in the III-V Compounds," Semiconductors and Semimetals, Volume 2, edited by R. K. Willardson and Albert C. Beer. New York: Academic Press, 1966.

14. Gibbons, James F. "Ion Implantation in Semiconductors - Part I Range Distribution Theory and Experiments," Proceedings of the IEEE, 56(3):295-319 (March 1968).

15. Gibbons, James F. Projected Range Statistics. Stroudsburg, Pa.: Dowden, Hutchison and Rose, Inc., 1975.

16. Iida, Shinya and Kazuhiro Ito. "Selective Etching of Gallium Arsenide Crystals in H_2SO_4 -H_2O_2 -H_2O System," Journal of the Electrochemical Society: Solid State Science, 118(5):768 (May 1971).

17. Key, M. V. Photoluminescence Study of Ion Implantation Damage in Gallium Arsenide. Unpublished MS thesis. Wright-Patterson Air Force Base, Ohio: Air Force Institute of Technology, December 1981.

18. Kittel, C. Introduction to Solid State Physics. New York: John Wiley and Sons, 1971.

19. Kolthoff, K. M., et al. Volumetric Analysis. Volume 3, New York: Interscience Publishers, Inc., 1957.

20. Lindhard, J., et al. "Range Concepts and Heavy Ion Ranges," Mat. Fys. Medd. Dan. Vid.,Sclsk 33:1 (1963).

21. Maclin, M. T. Depth-Resolved Luminescence of Gallium Arsenide using Ion Etching. Unpublished MS thesis. Wright-Patterson Air Force Base, Ohio: Air Force Institute of Technology, December 1981.

22. Martinelli, R. U. and C. C. Wang. "Electron-beam Penetration in GaAs," Journal of Applied Physics, 44(7):3350-3351 (July 1975).

23. McKelvey, J. P. Solid State and Semiconductor Physics. New York: Harper and Row, 1966.

24. Morgan, D. V. "The Characterization and Application of Ion-Induced Damage in Gallium Arsenide Devices," Radiation Physics and Chemistry, 15(5):627-636 (March 1980).

25. Norris, C. B. and C. E. Barnes. "Cathodoluminescence Studies of Anomalous Ion Implantation Defect Introduction in Lightly and Heavily Doped Liquid Phase Epitaxial GaAs: Sn," Journal of Applied Physics, 51(11):5764-5772 (November 1980).

26. Pankove, Jacques I. Optical Processes in Semiconductors. Englewood Cliffs, NJ: Prentice-Hall, Inc., 1971.

27. Pierce, B. J. Luminescence and Hall Effects of Ion Implanted Layers of ZnO. Unpublished dissertation. Wright-Patterson Air Force Base, Ohio: Air Force Institute of Technology, September 1974.

28. Seki, Y., et al. "Properties of Epitaxial GaAs Layers from a Triethyl Gallium and Arsine System," Journal of Electrochemical Society: Solid-State Science and Technology, 122(8):1108-1112 (August 1975).

29. Sturge, M. D. "Optical Absorption of Gallium Arsenide Between 0.6 and 2.75 eV," Physical Review, 127(3):768-773 (August 1962).

30. Williams, E. W. and C. T. Elliott. "Luminescence Studies of a New Line Associated with Germanium in GaAs," British Journal of Applied Physics, 2(2):1657-1665 (February 1969).

31. Williams, E. W., et al. "Photoluminescence II: Gallium Arsenide," Semiconductors and Semimetals, Volume 8, edited by R. K. Willardson and Albert C. Beer. New York: Academic Press, 1972.

Appendix

Luminescence Spectra of Samples

Prior to Etching

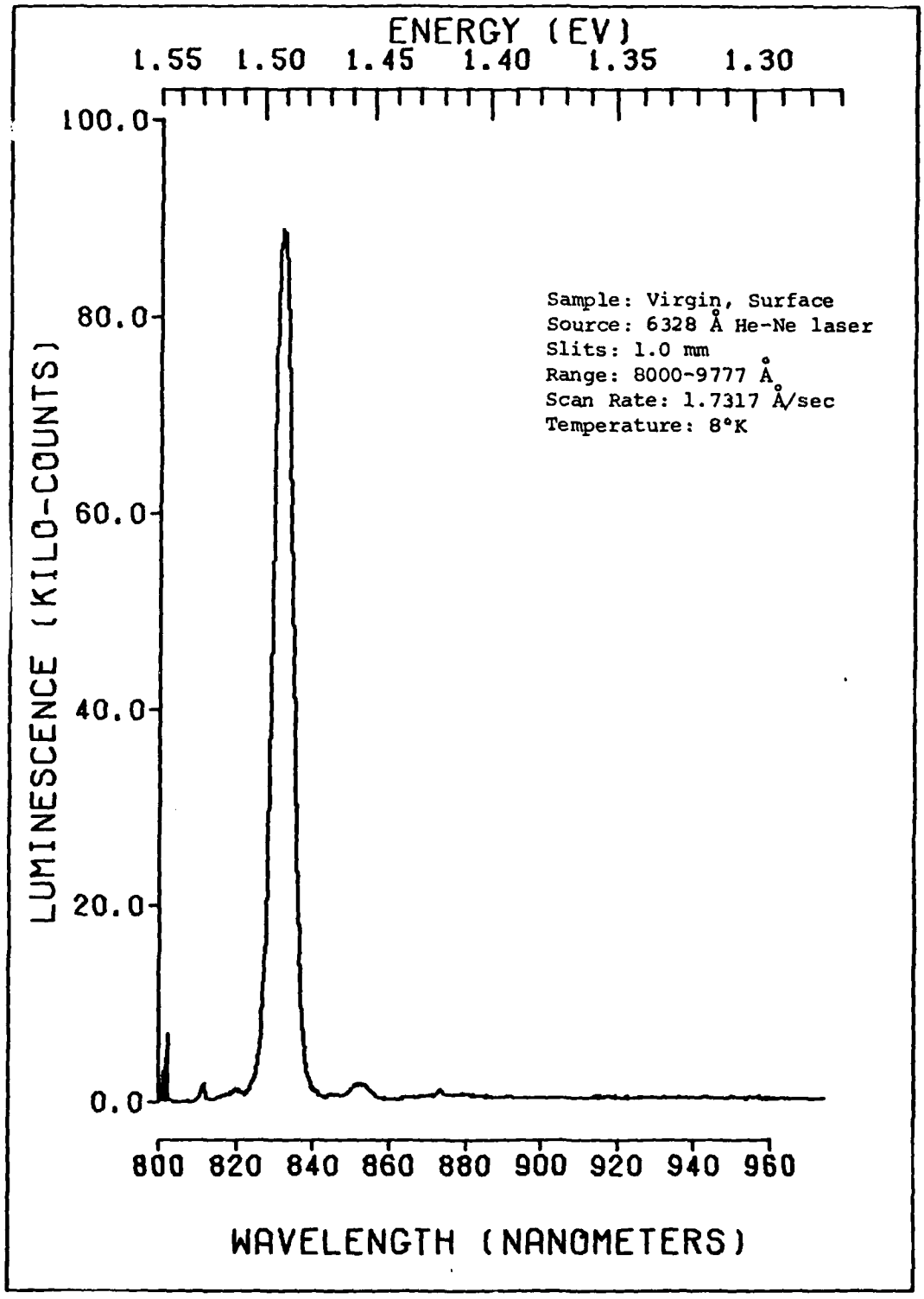

Fig. A-1. Surface Photoluminescence Spectrum of Virgin GaAs

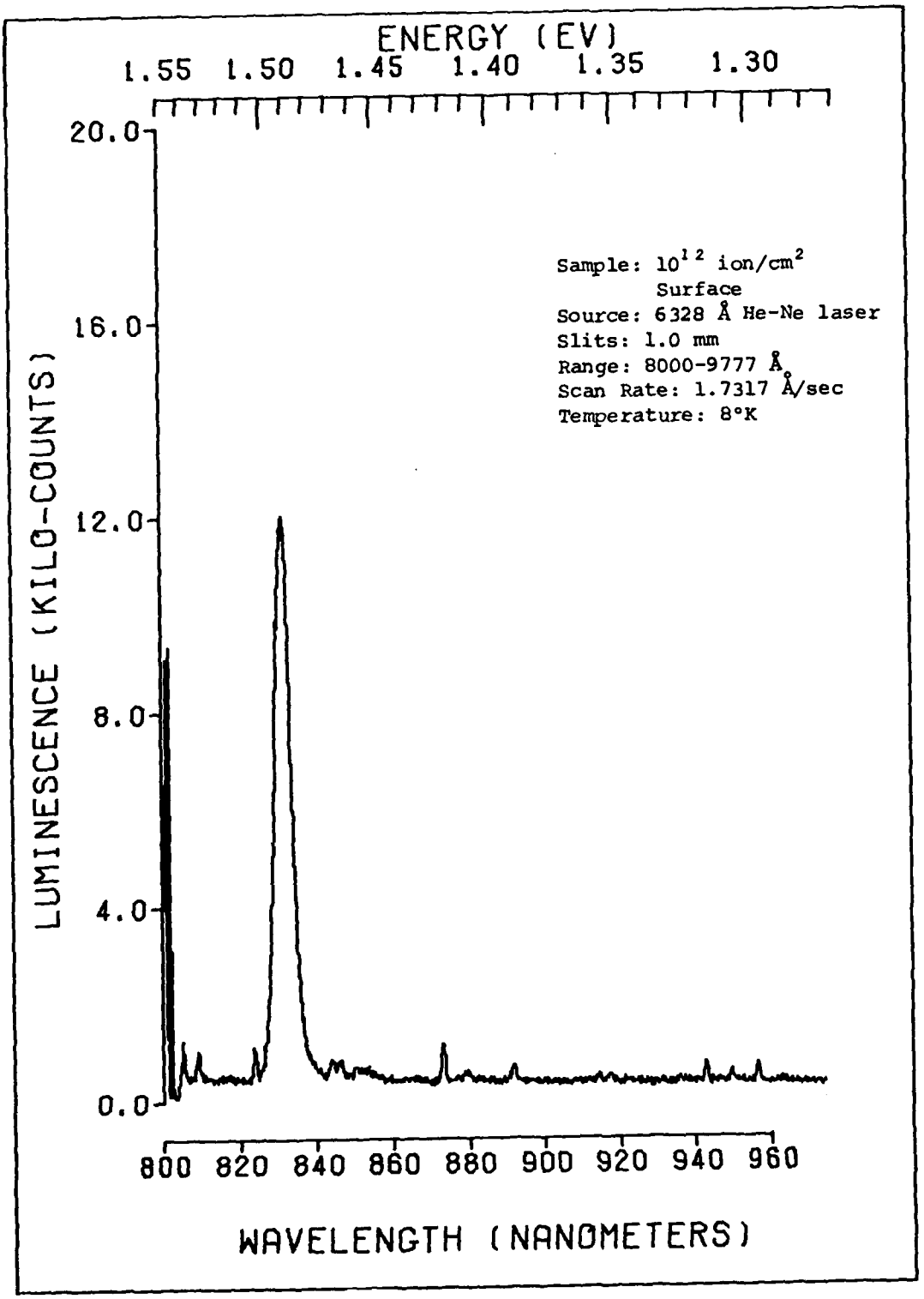

Fig. A-2. Surface Photoluminescence Spectrum of Si Implanted (10^{12} ion/cm^2) GaAs

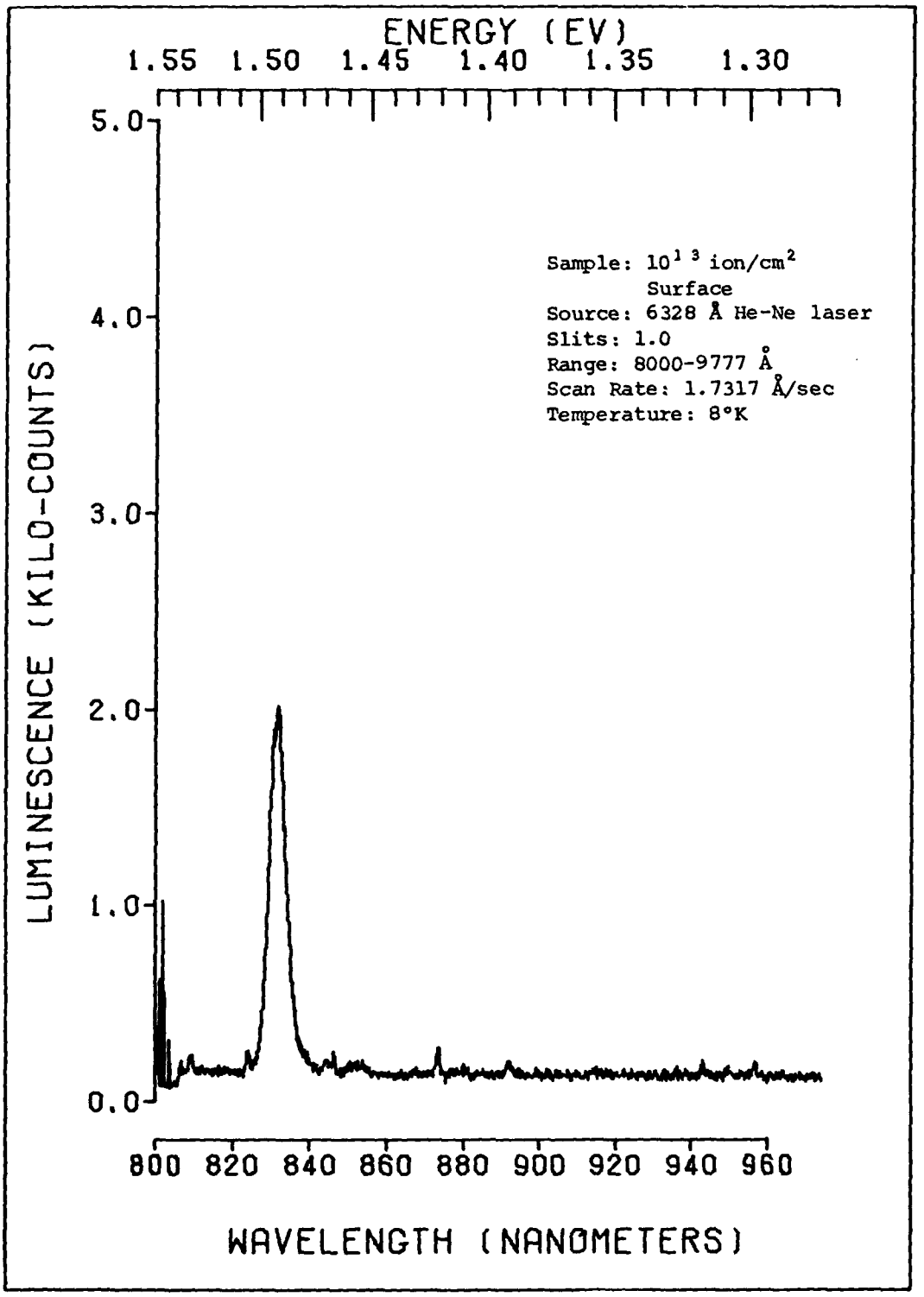

Fig. A-3. Surface Photoluminescence Spectrum of Si Implanted (10^{13} ion/cm^2) GaAs

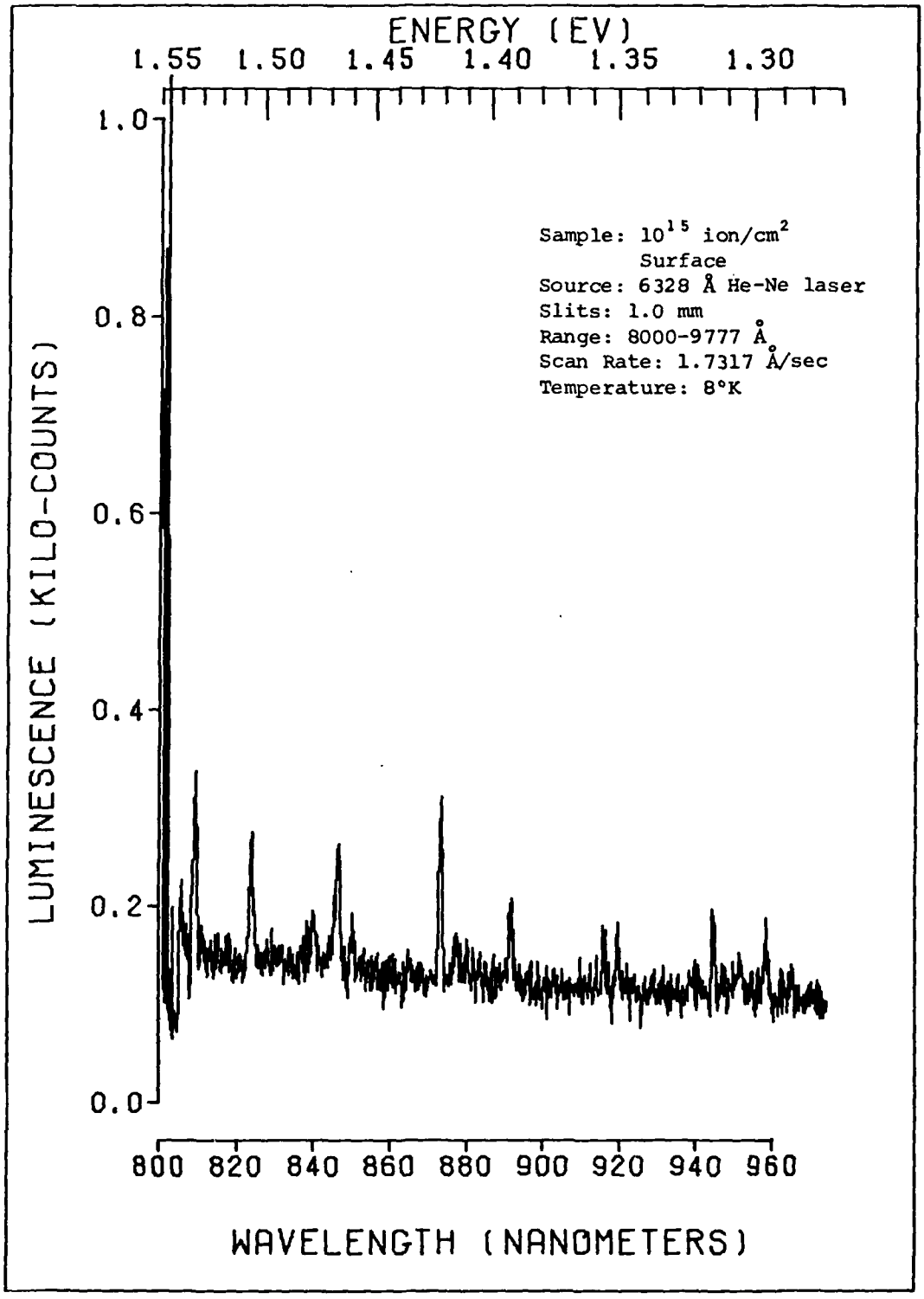

Fig. A-4. Surface Photoluminescence Spectrum of Si Implanted (10^{15} ion/cm^2) GaAs

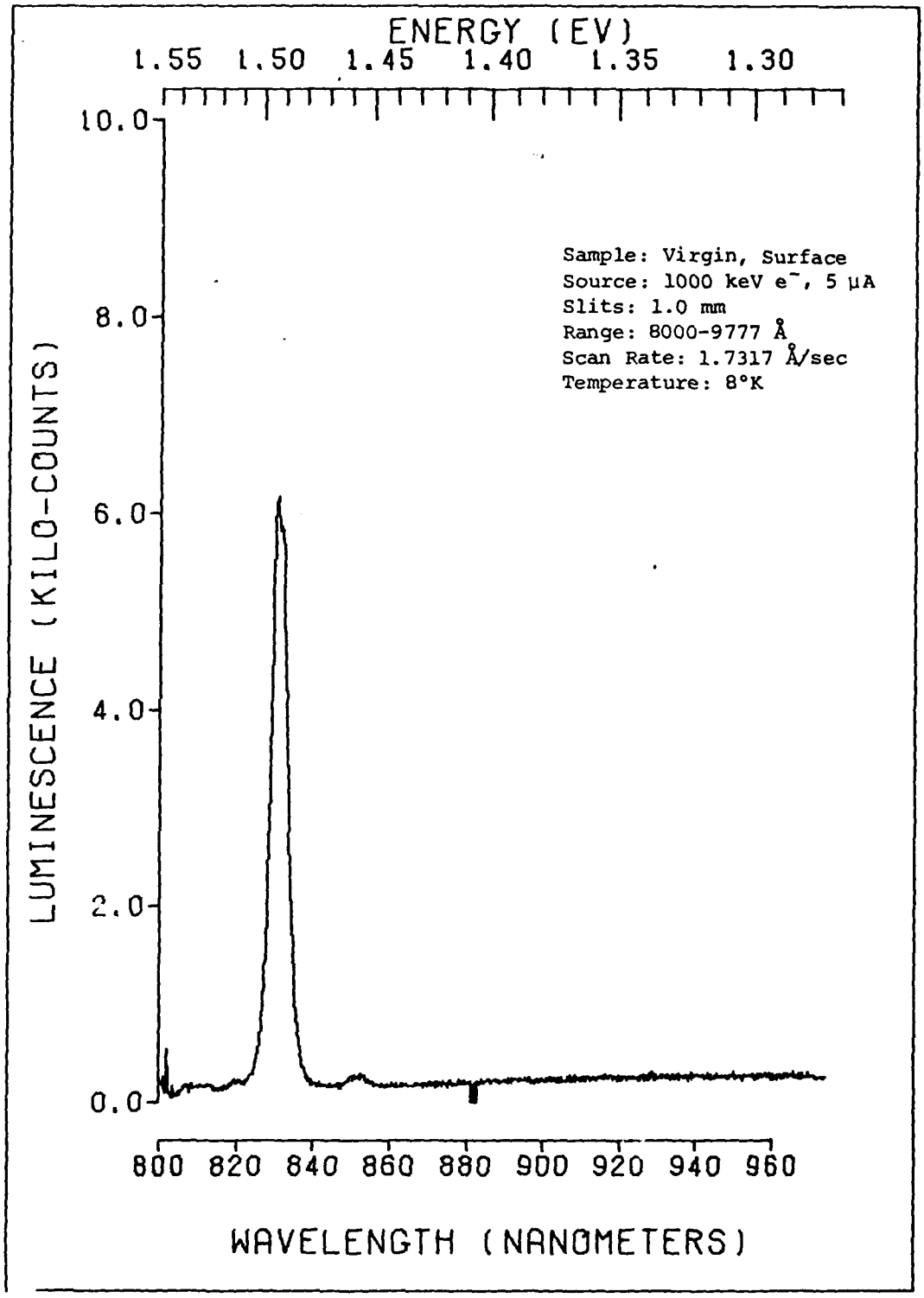

Fig. A-5. Surface Cathodoluminescence Spectrum of Virgin GaAs

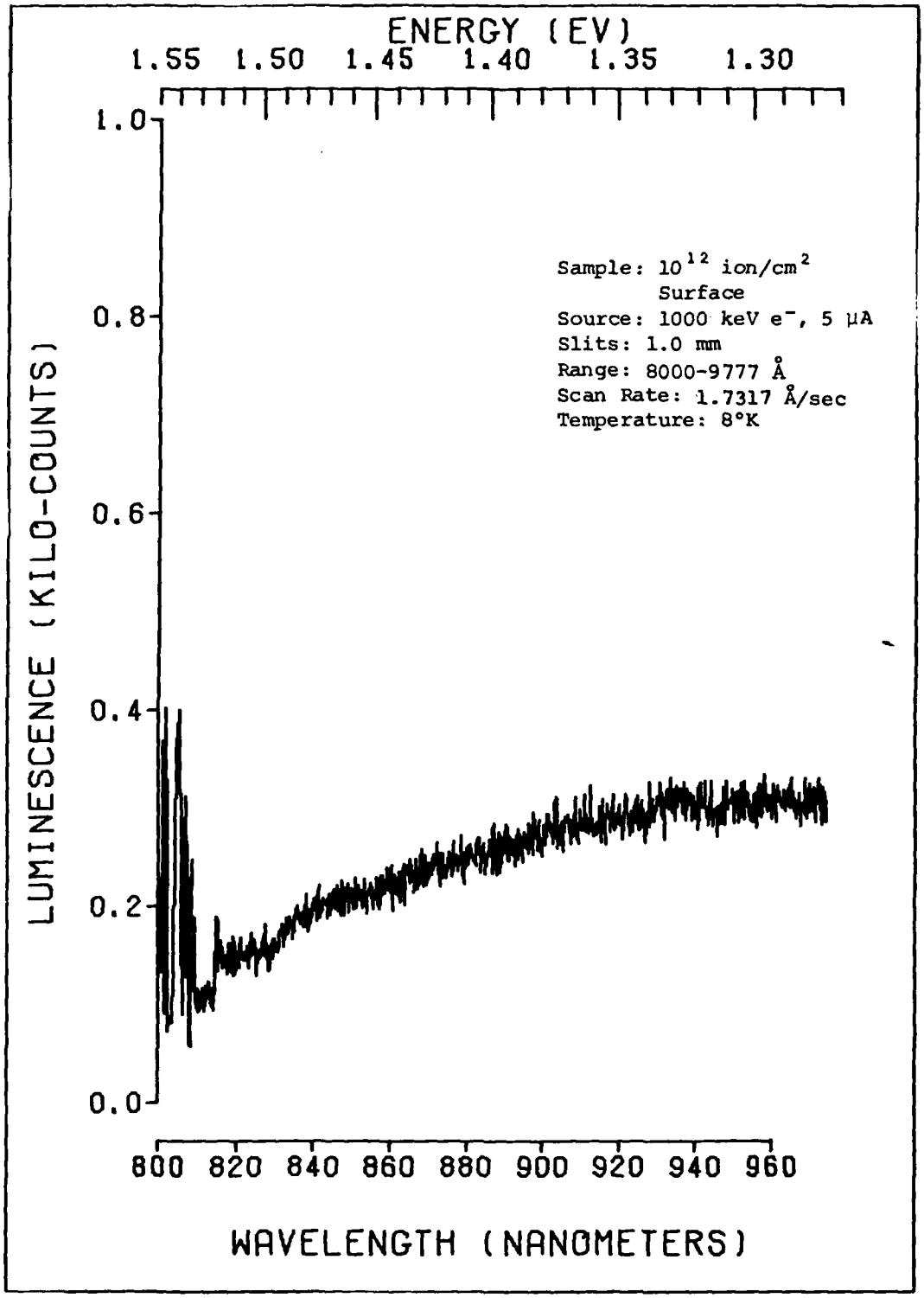

Fig. A-6. Surface Cathodoluminescence Spectrum of Si Implanted (10^{12} ion/cm^2) GaAs.

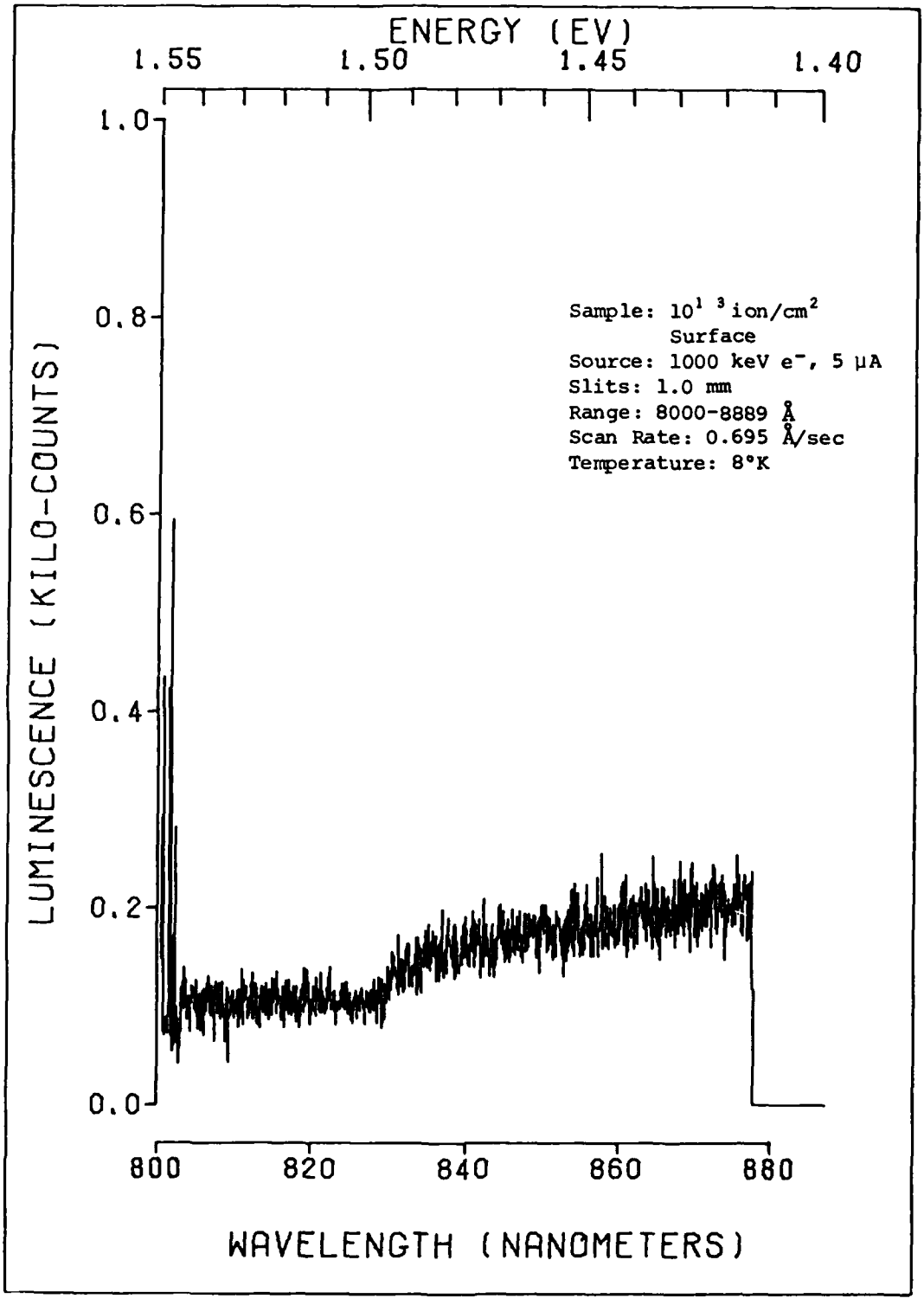

Fig. A-7. Surface Cathodoluminescence Spectrum of Si Implanted (10^{13} ion/cm^2) GaAs

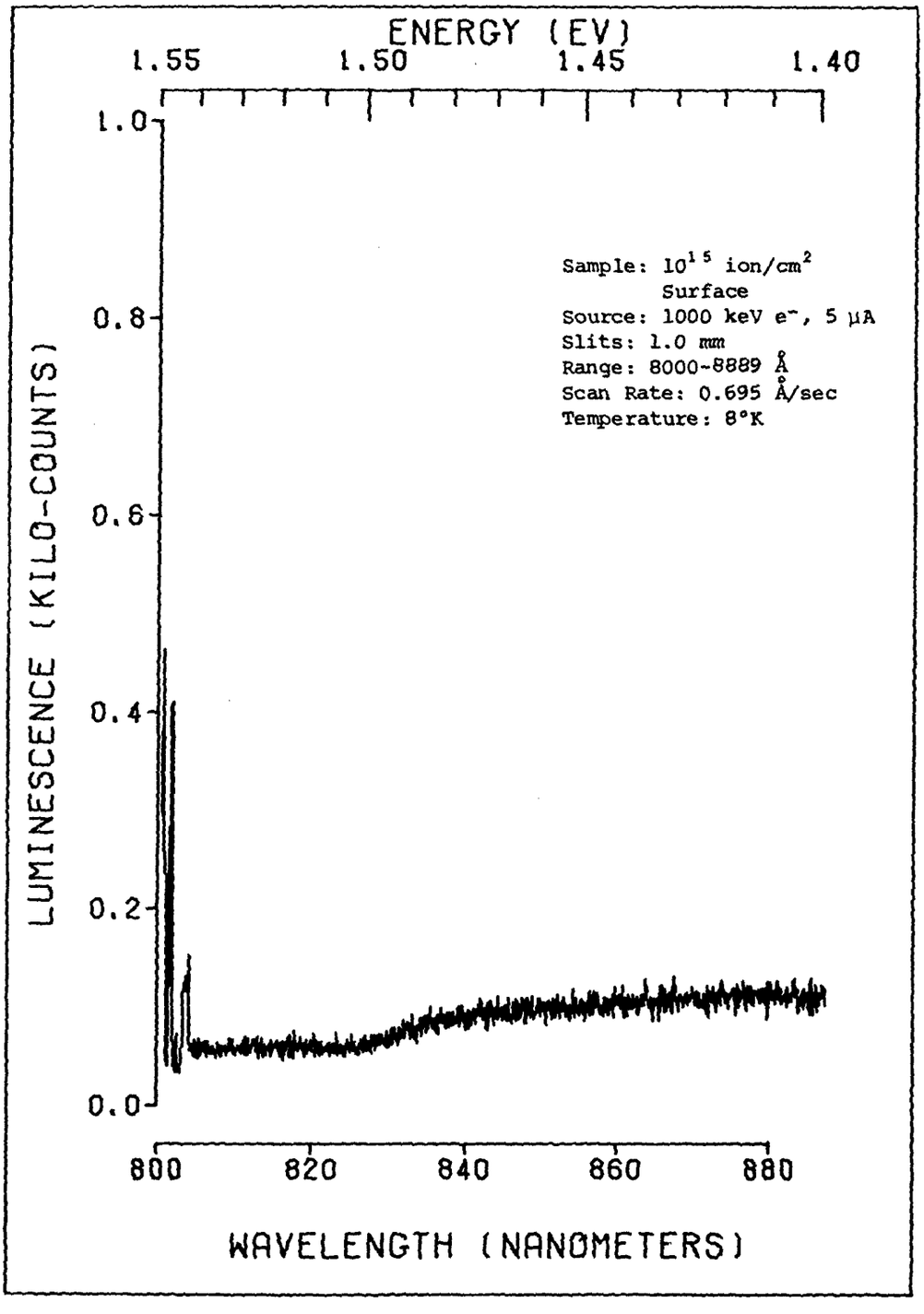

Fig. A-8. Surface Cathodoluminescence Spectrum of Si Implanted (10^{15} ion/cm^2) GaAs

Vita

PII Redacted

Daniel Lee DeForest [redacted]. He spent his childhood and early adult years in Houston, where he attended J. Frank Dobie High School. During this time he was involved in band and junior AFROTC. He also attained the rank of Eagle Scout while a member of the Boy Scouts of America. In 1976 he finished high school and entered Baylor University in Waco, Texas on a full AFROTC scholarship. He participated in the honors program there while majoring in Chemistry. He was also a member of the James Connally Squadron of the Arnold Air Society. During his senior year his AAS chapter hosted the national convention of which he was Deputy Commander. Upon graduation Cum Laude from Baylor in 1980, he entered the USAF in May 1980 and proceeded to attend the Air Force Institute of Technology in pursuit of a Masters of Science degree in Nuclear Engineering.

SECURITY CLASSIFICATION OF THIS PAGE (When Data Entered)

REPORT DOCUMENTATION PAGE	READ INSTRUCTIONS BEFORE COMPLETING FORM
1. REPORT NUMBER	2. GOVT ACCESSION NO. AD-A115 487 / 3. RECIPIENT'S CATALOG NUMBER
4. TITLE (and Subtitle) CATHODOLUMINESCENCE AND PHOTOLUMINESCENCE STUDY OF SILICON IMPLANTED GALLIUM ARSENIDE	5. TYPE OF REPORT & PERIOD COVERED
	6. PERFORMING ORG. REPORT NUMBER
7. AUTHOR(s) Daniel L. DeForest, Air Force Institute of Technology	8. CONTRACT OR GRANT NUMBER(s)
9. PERFORMING ORGANIZATION NAME AND ADDRESS Air Force Institute of Technology (AFIT/ENA) Wright Patterson AFB, Ohio 45433	10. PROGRAM ELEMENT, PROJECT, TASK AREA & WORK UNIT NUMBERS
11. CONTROLLING OFFICE NAME AND ADDRESS AFIT/ENA	12. REPORT DATE March 1982
	13. NUMBER OF PAGES 72
14. MONITORING AGENCY NAME & ADDRESS(if different from Controlling Office)	15. SECURITY CLASS. (of this report) Unclassified
	15a. DECLASSIFICATION DOWNGRADING SCHEDULE

16. DISTRIBUTION STATEMENT (of this Report)

Approved for public release; distribution unlimited

17. DISTRIBUTION STATEMENT (of the abstract entered in Block 20, if different from Report)

18. SUPPLEMENTARY NOTES

APPROVED FOR PUBLIC RELEASE: AFR 190-17.

15 APR 1982

Lynn E. Wolaver
Dean for Research and Professional Development
Air Force Institute of Technology (ATC)
Wright-Patterson AFB, OH 45433

19. KEY WORDS (Continue on reverse side if necessary and identify by block number)

Gallium arsenide; Depth profile; Ion implantation; Chemical etching; Silicon implant

20. ABSTRACT (Continue on reverse side if necessary and identify by block number)

Depth resolved photoluminescence and cathodoluminescence data were obtained from gallium arsenide implanted with 120 keV silicon ions. The luminescence data were studied as a function of depth in am effort to determine the implant damage profile of the silicon in GaAs. A chemical etchant was used to etch off successive layers of the crystal surface. The substrate material used for this study was bulk GaAs, grown by the Liquid-Encapsulated Czochralski (LEC) method.

DD FORM 1 JAN 73 1473 EDITION OF 1 NOV 65 IS OBSOLETE

SECURITY CLASSIFICATION OF THIS PAGE (When Data Entered)

The data from both photo- and cathodoluminescence indicated that the extent of damage produced in the samples increased with increasing dosage. This is supported by similar studies involving implanted GaAs. Additionally, a "dead" layer, in which all cathodoluminescence was completely quenched, was observed extending up to depths of 3500 Å into the samples. Correlation of the data from all implanted samples indicated that either some diffusion of defects had occurred or that the theory predicting the implant profile is flawed.